PHYSICAL REVIEW D **90,** 035024 (2014)

Raising the Higgs mass in supersymmetry with $t - t'$ mixing

Cyrus Faroughy[*] and Kevin Grizzard[†]

Department of Physics and Astronomy, Johns Hopkins University, Baltimore, Maryland 21218, USA

(Received 19 May 2014; published 29 August 2014)

In this article we propose a new strategy to address the little hierarchy problem. We show that the addition of a fourth generation with vectorlike quarks to the minimal supersymmetric standard model can raise the predicted value of the physical Higgs mass by mixing with the top sector. The mixing requires a larger top quark Yukawa coupling (by up to ∼6%) to produce the same top mass. Since loop corrections to m_h go as y_{top}^4, this will in turn increase the predicted value of the physical Higgs mass, a point not previously emphasized in the literature. In the presence of mixing, for A terms and soft masses around 900 GeV, a Higgs mass of 125 GeV can be generated while retaining perturbativity of the gauge couplings, evading constraints from electroweak precision measurements and recent LHC searches, and pushing the Landau pole for the top Yukawa above the GUT scale. Soft masses can be as low as 800 GeV in parts of parameter space with a Landau pole at $\sim 10^{10}$ GeV. However, the Landau pole can still be pushed above the GUT scale if one sacrifices perturbative unification by adding fields in a $\mathbf{5} + \bar{\mathbf{5}}$ representation. With a ratio of weak-scale vector masses $\neq 1$, soft masses may be slightly below 800 GeV. The model predicts new quarks and squarks with masses $\gtrapprox 750$ GeV. We briefly discuss potential paths for discovery or exclusion at the LHC.

DOI: 10.1103/PhysRevD.90.035024 PACS numbers: 12.60.Jv

I. INTRODUCTION

Dynamically broken supersymmetry offers an elegant way of cutting off leading divergences of quantum corrections to the Higgs mass parameter in the standard model. Unless parameters in the model are finely tuned, one expects that the mass of supersymmetric particles are of the same order as the Z and W masses. In particular, quantum corrections to the Higgs mass parameter are dominated by the contributions from the top quark, because of the large Yukawa coupling. To preserve naturalness, this leads to the expectation that the top squark should be relatively light.

However, results from the Large Hadron Collider (LHC) indicate that the Higgs mass is ∼125 GeV [1,2]. In the minimal supersymmetric standard model (MSSM), a mass so much higher than the tree-level upper bound of m_Z can be accommodated only with extremely heavy top squarks, or moderately heavy top squarks and large top squark mixing. The quadratic divergence contributed by such a heavy top squark then needs to be canceled at the level of $\sim 10^{-4}$, leading to a significantly fine-tuned theory. This tuning is significantly worse than the tuning implied by direct constraints on superpartners at the LHC. In fact, in the case of only moderate mixing, the top squark mass implied by this Higgs mass is higher than the direct collider limit ∼3 TeV that can ever be set by the LHC.

Unlike many other experimental constraints on the MSSM, this "little hierarchy" problem [3,4] is directly associated with the low energy spectrum of the theory. Consequently, it cannot be solved through ultraviolet mechanisms that are often invoked to address indirect constraints (such as flavor or CP violation; see [5] for an overview) or alteration of the collider signatures of supersymmetry to avoid direct constraints on the theory [6–11]. Several attempts have been made to modify the MSSM spectrum through the addition of matter fields to raise the Higgs mass [12–45]. These mechanisms were originally proposed to accommodate the Higgs mass bound $\gtrapprox 114$ GeV imposed by LEP, and though more recent work has demonstrated the ability for such a mechanism to yield a Higgs mass ∼125 GeV (e.g., [46]), in general the higher mass needs significantly larger couplings than considered in the earlier models, leading to the rapid appearance of Landau poles marginally above the weak scale. While such a possibility cannot be logically excluded, it destroys the success of perturbative grand unification in supersymmetric models, an aesthetic success of the MSSM.

In this paper, we propose a new strategy to address the little hierarchy problem. The largest loop contribution to the effective potential of the Higgs comes from the top supermultiplet and the magnitude of this contribution is governed by the top Yukawa. The Yukawa coupling used in current estimates of the top quark contribution to the Higgs mass is directly extracted from measurements of the top mass. However, the naive relation between the physical mass of the top quark and the Yukawa coupling, extracted from the tree level Lagrangian, is modified when the top supermultiplet is mixed with other heavier states. When diagonalizing the mass matrix, the new mixing terms will contribute negatively to the naive estimate $y_t v \sin\beta$, thus

[*]cfarough@pha.jhu.edu
[†]kgrizz@pha.jhu.edu

TABLE I. The third and fourth generation colored fields and their quantum numbers in the gauge-eigenstate basis are listed in the table above. We follow the standard convention that all chiral supermultiplets are defined in terms of two-component left-handed Weyl spinors, so that charge conjugates of right-handed fields are used. The barred fields denote gauge-eigenstate fields belonging to the $\overline{\mathbf{10}}$ representation of $SU(5)$. Four-component Dirac fermions can be constructed as $q_D = (q_i, q_i^{c\dagger})^T$. The mass basis fermions are the top t, bottom b, and the new quarks $t'_{1,2}$ and b' of charge $+2/3$ and $-1/3$, respectively. Their superpartners are the top squarks $\tilde{t}_{1,2}$, sbottoms $\tilde{b}_{1,2}$, and the corresponding non-MSSM squarks $\tilde{t}'_{1,2,3,4}$ and $\tilde{b}'_{1,2}$.

Supermultiplet	Scalars	Fermions	$SU(3)_C$	$SU(2)_L$	$U(1)_Y$	T^3	Q
Q_3	$(\tilde{u}_3, \tilde{d}_3)$	(u_3, d_3)	**3**	**2**	1/6	(1/2, −1/2)	(2/3, −1/3)
U_3^c	$\tilde{u}_3^c$	u_3^c	$\bar{\mathbf{3}}$	**1**	−2/3	0	−2/3
D_3^c	$\tilde{d}_3^c$	d_3^c	$\bar{\mathbf{3}}$	**1**	1/3	0	1/3
Q_4	$(\tilde{u}_4, \tilde{d}_4)$	(u_4, d_4)	**3**	**2**	1/6	(1/2, −1/2)	(2/3, −1/3)
U_4^c	$\tilde{u}_4^c$	u_4^c	$\bar{\mathbf{3}}$	**1**	−2/3	0	−2/3
$\bar{Q}_4^c$	$(\tilde{\bar{d}}_4^c, \tilde{\bar{u}}_4^c)$	$(\bar{d}_4^c, \bar{u}_4^c)$	$\bar{\mathbf{3}}$	**2**	−1/6	(1/2, −1/2)	(1/3, −2/3)
$\bar{U}_4$	$\tilde{\bar{u}}_4$	$\bar{u}_4$	**3**	**1**	2/3	0	2/3

requiring a larger Yukawa coupling to obtain the measured value of the top, $m_t \sim 173$ GeV. Since the Higgs effective potential depends upon the fourth power of this coupling, even a moderate increase can lead to a significant enhancement of the Higgs mass.

We demonstrate this mechanism through a simple extension of the models [38,39,46] where a vectorlike fourth generation with Yukawa couplings to the Higgs was introduced. In these models, the additional contributions from the vectorlike generation were sufficient to push the Higgs mass above the LEP bound of ∼114 GeV. This goal could be accommodated with perturbative gauge coupling unification with relative ease using only the Yukawa couplings of the fourth generation with itself. Consequently, mixing between the fourth generation and the standard model was not explored. But the mixing between the top quark and the fourth generation is experimentally fairly unconstrained. Indeed, recently there has been more interest shown in exploring this possibility, with [47] in particular seeking to constrain the possible dominant mixing angle for any (single) vectorlike heavy multiplet. However, it has not been noted that such a mixing can contribute significantly to the mechanism for raising m_h so far above m_Z. When this mixing is $\mathcal{O}(1)$, we show that the Yukawa couplings necessary to obtain the physical top quark mass are large enough to substantially increase the Higgs mass.

This paper is structured as follows. We describe the model in Sec. II. In Sec. III, we discuss the effects of large mixing on the top Yukawa. We compute the weak-scale mixing Yukawa couplings necessary to achieve a Higgs mass of ∼125 GeV and the induced top Yukawa Landau pole. In Sec. IV we study the experimental constraints and briefly discuss the LHC phenomenology. Finally, we conclude in Sec. V.

II. THE MODEL

In this model, we extend the MSSM by adding a full vectorlike fourth generation (i.e., a chiral fourth generation plus its mirror) with Yukawa couplings to the Higgs. Furthermore, the couplings mixing the fourth generation and the top sector are allowed to take on values close to unity; they have a quasifixed point which limits their TeV values to be not much larger than 1 [39]. However, we ignore mixing with the first and second generations since these are constrained by experiment to be small. We consider the simplest model which preserves gauge coupling unification. Therefore, the new vectorlike generation contains quark and lepton supermultiplets Q_4, U_4^c and E_4^c, living in the **10** representation of SU(5), plus the corresponding mirror generation $\bar{Q}_4^c$, $\bar{U}_4$, and $\bar{E}_4$ living in the $\overline{\mathbf{10}}$ representation. The $SU(3)_c \times SU(2)_L \times U(1)_Y$ quantum numbers of the additional colored superfields and the top sector, plus explanation of our conventions and notation, are shown in Table I.

The relevant mass-eigenstate Dirac fermions are the top t, bottom b, and the new quarks $t'_{1,2}$ and b' of charge $+2/3$ and $-1/3$, respectively. In the scalar sector the relevant particles are the top squarks $\tilde{t}_{1,2}$, sbottoms $\tilde{b}_{1,2}$, and the corresponding non-MSSM squarks $\tilde{t}'_{1,2,3,4}$ and $\tilde{b}'_{1,2}$. The terms in the superpotential that affect the Higgs mass are

$$W \subset y_{ij} Q_i H_u U_j^c + \mu_Q \bar{Q}_4^c Q_4 + \mu_U \bar{U}_4 U_4^c + \mu H_u H_d \qquad (1)$$

where i and j are generation indices than run from 3 to 4, and μ is the usual coefficient of the Higgs bilinear term. Terms such as $\mu_{34} Q_3 \bar{Q}_4^c$ are rotated away without loss of generality. Yukawa couplings of the form $\bar{y}_{44} H_d \bar{Q}_4^c \bar{U}_4$ and Yukawa couplings between the Higgs and the leptons are ignored since their effect in raising the Higgs mass is subdominant in the large $\tan\beta$ limit. In the soft Lagrangian, we assume the same squared mass Δm^2 for all the squarks, $B\mu$ terms corresponding to each vectorlike mass (ignoring mixed $B\mu$ terms with the third generation), and A terms of the form $y_{ij} A$ associated with each Yukawa coupling. Throughout the paper, we set $\tan\beta = 30$. We refer to the

Appendixes for details about the particle spectrum and the interaction Lagrangian.

III. THE EFFECTS FROM MIXING

A. Mixing and the top Yukawa coupling

As stated in the introduction, the qualitative difference between this note and earlier work [38,39,46] is the emphasis on the mixing terms proportional to y_{34} and y_{43}. In general, we assume a parameter space where y_{34}, y_{43} and y_{44} are allowed to vary from 0 to values $\gtrsim 1$, while the top Yukawa is constrained to give the right top mass. We consider the four following benchmark scenarios for the Yukawas: (1) $y_{34} = -y_{43} \gg y_{44}$, (2) $y_{43} \gg y_{34}, y_{44}$, (3) $y_{34} \gg y_{43}, y_{44}$, and (4) $y_{44} \gg y_{34}, y_{43}$. Case 1 focuses on effects where both mixing Yukawas are significant, whereas cases 2 and 3 focus on mixing from only one term. Case 4 corresponds to earlier work [38,39,46] where the mixing terms y_{34} and y_{43} were ignored, and serves as a useful comparison. As will be shown in Sec. III B, the parameter space where this model makes sizable contributions to the Higgs mass is a region where the fourth generation is accessible at the LHC.

When mixing terms are present, and if $y_{44} = 0$, the top Yukawa coupling y_{33} necessary to obtain the measured top mass $m_t = 172.9$ GeV is given by

$$y_{33} = \frac{m_t}{v \sin\beta}\left(1 + \frac{(y_{43} v \sin\beta)^2}{\mu_Q^2 - m_t^2}\right)^{1/2}\left(1 + \frac{(y_{34} v \sin\beta)^2}{\mu_U^2 - m_t^2}\right)^{1/2}. \tag{2}$$

This formula is exact when $y_{44} = 0$ and is obtained after bidiagonalizing the up-type fermion mass matrix m_f^u (shown explicitly in Appendix A), identifying its smallest singular value with the top mass, and solving for y_{33}. If $y_{44} \neq 0$, the above formula still holds to a very good approximation since the coupling y_{44} first makes an appearance at fourth order in the expansion parameter $(v/\mu_{Q,U})$, and therefore has a negligible effect in raising the value of y_{33}.

For simplicity, we take $\mu_Q = \mu_U \equiv \mu_4$. In this case, we can define $\Delta = v/\mu_4$ to quantify the hierarchy between the new vectorlike mass scale and the electroweak scale, such that $\Delta = 0$ in the limit $\mu_4 \to \infty$. At large $\tan\beta$, and taking $m_t/v = 1$, Eq. (2) can be approximated as

$$y_{33} \approx 1 + \frac{1}{2}\left(\frac{\Delta^2}{1-\Delta^2}\right)(y_{43}^2 + y_{34}^2) + \mathcal{O}(\Delta^4). \tag{3}$$

Evidently, $\Delta > 0$ leads to an increase in the top Yukawa. As a result, the soft masses Δm needed to get a 125 GeV Higgs decrease. Taking the value of the mass of the new quarks to be near their experimental limit of 700–800 GeV (see Sec. IV C) leads to the constraint $\Delta \lesssim 1/4$. Then, in the case where the mixing Yukawas are near unity, the effects of mixing between the top sector and the fourth generation can lead to an increase of y_{33} by about 6%. This can significantly increase the Higgs mass squared since the radiative corrections go as y_{33}^4. Mixing effects on the Higgs mass are studied in detail in Sec. III B. Lastly, we note that an increase in the top Yukawa also leads to an increase in the Higgs quartic; however, this increase is subdominant compared to the Higgs mass.

B. Weak-scale Yukawa couplings

In this section we compute the weak-scale Yukawa couplings necessary to obtain the required Higgs mass using the one-loop effective potential in the decoupling limit (where $m_A, m_{H^+}, m_{H^-}, m_{H^0} \gg m_h$). Contributions to the Higgs effective potential have the following form:

$$\Delta V = \frac{3}{32\pi^2}\left[\sum_{\{\tilde{m}_a\}} \tilde{m}_a^2\left(\ln\frac{\tilde{m}_a^2}{Q^2} - \frac{3}{2}\right) - 2\sum_{\{m_a\}} m_a^2\left(\ln\frac{m_a^2}{Q^2} - \frac{3}{2}\right)\right] \tag{4}$$

where Q is the renormalization scale and m_a ($\tilde{m}_a$) are the quark (squark) masses. The summation runs over the masses of the heavy up-type quarks ($a = t, t_1', t_2'$) and their superpartners ($a = \tilde{t}_{1,2}, \tilde{t}'_{1,2,3,4}$). The resulting physical Higgs mass is then

$$m_h = \sqrt{m_Z^2 \cos^2 2\beta + \frac{1}{2}\left(\frac{\partial^2(\Delta V)}{\partial v_u^2} - \frac{1}{v_u}\frac{\partial(\Delta V)}{\partial v_u}\right)}. \tag{5}$$

For numerical efficiency, the algorithm used to solve for the necessary parameters obtains a Higgs mass in the range 125.5 ± 0.5 GeV. For this set of computations we take the soft terms to be of the form $\Delta m = A$, as might be expected in gravity mediation (or high scale gauge mediation [38]), and choose $\mu_4 = 900$ GeV. The Yukawa values at the weak scale as functions of the soft masses are plotted in Fig. 1, along with their constraints from electroweak precision measurements. As one would intuitively expect, the mixing Yukawas necessary to achieve a given Higgs mass are smaller when $|y_{34}| \sim |y_{43}|$ than when one of these couplings dominates the other. However, the lowest possible value of Δm consistent with electroweak precision measurements (EWPM) is $\Delta m \sim 800$ GeV and occurs for the case where $y_{34} \sim 0.8$ and $y_{43} = y_{44} = 0$.

C. Top Yukawa Landau pole

The mixing terms y_{34} and y_{43} significantly affect the Higgs mass only when they are $\mathcal{O}(1)$. These $\mathcal{O}(1)$ Yukawas affect the renormalization group evolution of the top Yukawa y_{33} and can cause it to hit a Landau pole. In this section, we estimate the scale at which this Landau pole is attained for various choices of the Yukawas and soft terms

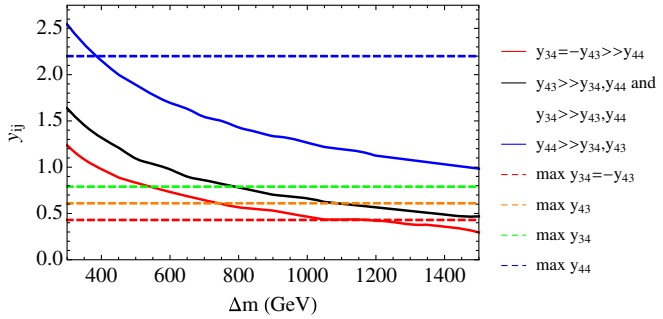

FIG. 1 (color online). We plot the values of the Yukawa couplings at the weak scale necessary to obtain $m_h = 125.5 \pm 0.5$ GeV, as a function of Δm. We take $A = \Delta m$, $\mu_4 = 900$ GeV. When either y_{34} or y_{43} dominates, the same value of the dominant Yukawa is required to get $m_h = 125.5$ GeV so both scenarios are represented by one black line. The dotted lines show the maximum values allowed by EWPM for each mixing scenario (see Sec. IV). Since y_{34} and y_{43} contribute to the oblique parameters differently they have different constraints on their maximum values, represented by the green and orange dotted lines, respectively. Above the dotted line requires Yukawas larger than allowed by EWPM and is thus ruled out.

necessary to obtain a Higgs mass ~125 GeV. The top Yukawa two-loop beta function presented in Appendix D is used to calculate the scale Λ where the coupling y_{33} hits a Landau pole. Below, we plot Λ as a function of the soft mass Δm and consider the effects from

(1) Different mixing scenarios.
(2) A terms.

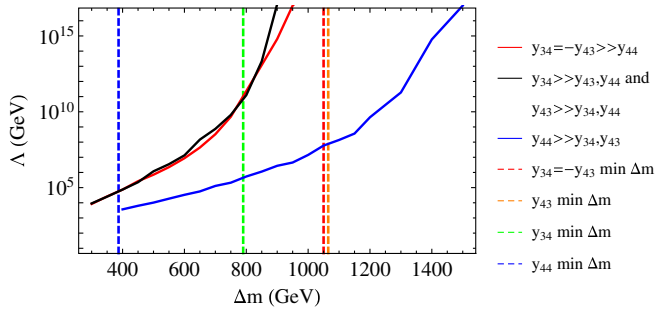

FIG. 2 (color online). We plot the scale Λ where the y_{33} required to get $m_h = 125.5$ GeV hits a Landau pole, as a function of the soft mass Δm. We set $A = \Delta m$, $\mu_4 = 900$ GeV, and $n_5 = 0$. Soft masses to the left of the dotted lines can only yield $m_h = 125.5$ GeV with Yukawa couplings larger than allowed by EWPM and are thus ruled out (see Sec. IV). Physically uninteresting values of $\Lambda < 1$ TeV are not plotted. The presence of mixing decreases significantly the value of the soft masses needed. As can be seen from the plot, the scale of the Landau pole in the cases with sizable mixing are all comparable. The cases where either y_{34} or y_{43} dominate (shown in black) yield identical values since each contributes to the top Yukawa beta function in the same way. However, their differing effects on the oblique parameters lead to different minimum values for the soft masses.

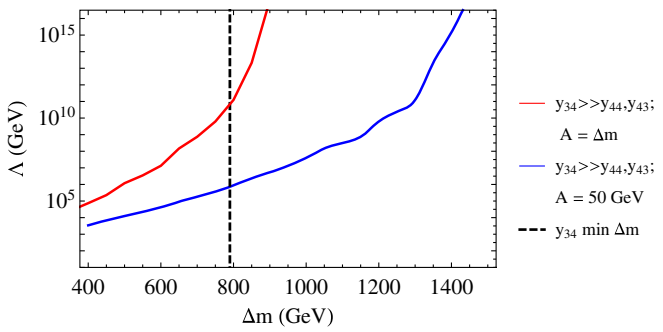

FIG. 3 (color online). We plot the scale Λ where the y_{33} required to get $m_h = 125.5$ GeV hits a Landau pole, as a function of the soft mass Δm. We set $y_{34} \gg y_{44}, y_{43}$, $\mu_4 = 900$ GeV, and $n_5 = 0$. Soft masses to the left of the dotted lines can only yield $m_h = 125.5$ GeV with Yukawa couplings larger than allowed by EWPM and are thus ruled out (see Sec. IV). There is only one line here since these limits are independent of the A terms). For a given soft mass the implied Landau pole gets significantly pushed up by the presence of A terms.

(3) The vectorlike mass μ_4.
(4) The number of extra multiplets in the $\mathbf{5} + \bar{\mathbf{5}}$ of SU(5).

From Fig. 2, we see that large mixing can push Λ above the GUT scale while retaining soft masses as low as ~900 GeV. The three different mixing scenarios give comparable results because these Yukawa couplings reinforce each other in their respective renormalization group evolution. In contrast, to push Λ above $\sim 10^{16}$ in the case with no mixing requires soft masses to be larger than 1.5 TeV.

From Figs. 3 and 4 it is clear that for a given soft mass, the implied Landau pole scale can also get pushed up by including larger A terms or a smaller vector mass. For $A = \Delta m \sim 900$ GeV, Λ can be pushed above the GUT

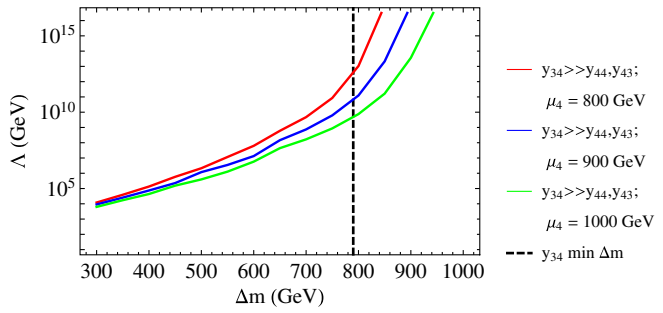

FIG. 4 (color online). We plot the scale Λ where the y_{33} required to get $m_h = 125.5$ GeV hits a Landau pole, as a function of the soft mass Δm. We set $y_{34} \gg y_{44}, y_{43}$, $A = \Delta m$, and $n_5 = 0$. Soft masses to the left of the dotted lines can only yield $m_h = 125.5$ GeV with Yukawa couplings larger than allowed by EWPM and are thus ruled out (see Sec. IV). For a given soft mass, the implied Landau pole increases as the vector mass decreases.

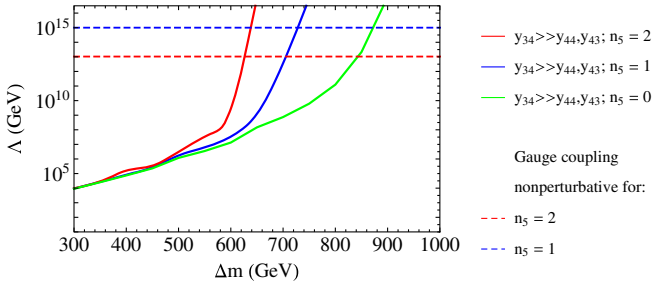

FIG. 5 (color online). We plot the scale Λ where the y_{33} required to get $m_h = 125.5$ GeV hits a Landau pole, as a function of the soft mass Δm. We set $y_{34} \gg y_{44}, y_{43}$, $A = \Delta m$, $\mu_4 = 900$ GeV. Here the dotted lines indicate where the gauge couplings become nonperturbative for $n_5 = 2$ and $n_5 = 1$. They remain perturbative all the way to the GUT scale for $n_5 = 0$.

scale. Δm can be as low as 800 GeV, albeit in parts of parameter space with a Landau pole at $\sim 10^{10}$ GeV.

In the last point (4) above, we included one more parameter in our analysis, namely, the number n_5 of multiplets in the $\mathbf{5} + \bar{\mathbf{5}}$ representation of $SU(5)$ that are added to the model. These could correspond, for example in the minimal version of gauge-mediated supersymmetry breaking, to messenger fields which do not couple to the Higgs and that communicate SUSY breaking from a hidden sector to the visible sector. This number does not affect the Yukawas necessary to obtain the Higgs mass but it contributes to the running of the gauge couplings, making them stronger in the ultraviolet. And since the gauge couplings contribute negatively to the renormalization of the Yukawas, a larger ultraviolet gauge coupling slows the growth of the y_{ij}'s, pushing up the Landau pole. However, as we will see, to preserve perturbative gauge coupling unification we cannot add an arbitrary number of n_5 in addition to the vectorlike $\mathbf{10} + \overline{\mathbf{10}}$ of SU(5) necessary in our model. To verify perturbativity we used the one-loop beta functions presented in Appendix D and required $g_{\text{unif}} \lesssim 3$. From Fig. 5, we see that the gauge couplings become nonperturbative around 10^{13} GeV for $n_5 = 2$ and 10^{15} GeV for $n_5 = 1$. They remain perturbative all the way to the GUT scale for $n_5 = 0$. Therefore, the Landau pole can still be pushed above the GUT scale if one sacrifices perturbativity at the scale of unification.

IV. CONSTRAINTS

In this section, we work out the constraints from Higgs production, measurements of V_{tb}^{CKM}, the most recent mass bounds from direct searches for vectorlike quarks at the LHC (with up to 19.5 fb^{-1} of 8 TeV data from CMS [48] and 14.3 fb^{-1} of 8 TeV data from the ATLAS detector) and constraints on the oblique parameters S and T [49] from electroweak precision measurements. We find that the oblique corrections and LHC direct searches place the dominant constraints on the total parameter space but that portions of the remaining parameter space available can still raise the Higgs mass to ~125 GeV while yielding new quarks discoverable at the LHC in the near future.

A. Higgs production

The Higgs production rate at the LHC is dominated by the gluon fusion process and recent measurements can be used to put constraints on any model with new particles that get their mass through the Higgs. In the case where a chiral fourth generation is added to the SM, this leads to an increase of the Higgs production rate by gluon fusion by about a factor of 9 over the SM rate, in contradiction with experiments. This is a result of the fact that the new quarks get all of their mass via coupling to the Higgs; no decoupling limit exists to ameliorate the situation. However, in the case of a new generation of vectorlike quarks the new quarks get their mass only partially through the Higgs, the remaining part coming from the vectorlike mass parameter(s), here μ_4. This opens the possibility that the new generation might contribute differently to Higgs production.

One can see the dependence of the relevant amplitude on the parameters of the model as follows. We take the large $\tan\beta$ limit throughout this discussion, though the procedure can be generalized in an obvious way. Consider an effective vertex coupling two gluons and a Higgs, which can be thought of as arising from a term in an effective Lagrangian with the form

$$\mathcal{L}_0 = g^* G_{\mu\nu} G^{\mu\nu} H, \tag{6}$$

where $H \to h + v$ after electroweak symmetry breaking (EWSB) so that $\mathcal{L}_0 \to \mathcal{L}_1 + \mathcal{L}_1'$, where

$$\mathcal{L}_1 = g^* G_{\mu\nu} G^{\mu\nu} h, \qquad \mathcal{L}_1' = g^* G_{\mu\nu} G^{\mu\nu} v. \tag{7}$$

The amplitude associated with the effective ggh vertex is simply the unknown g^*. This is the same amplitude as for the $\mathcal{L}_1'$ "vertex," which can be interpreted as a correction to the gluon self-energy Π^{gg}. In particular, it is that part of the self-energy that comes from the coupling of particles in the loop to the Higgs vacuum expectation value (we consider only the one-loop correction). Rather than directly computing the effective ggh coupling g^* by summing all one-loop $gg \to h$ diagrams, we can use the ggv coupling to obtain g^* from the well-known form of the gluon self-energy in a simple way. For this we need to consider all the contributions to the one-loop gluon self-energy, identify all the terms that include a factor of v, and sum the coefficients of v from each term. (Actually, what we need is just the sum, not individual coefficients.) Therefore to extract the information we want out of Π^{gg}, all we have to do is take a partial derivative with respect to v. In equation form, $g^* \sim \frac{\partial}{\partial v}[\Pi^{gg}(v)]$, where Π^{gg} is thought of as a function of v.

The form of corrections to vector boson propagators is well known. Since the coupling for a non-Abelian gauge theory is universal, all colored fermions in the loop contribute in the same way, i.e., the only difference between their contributions comes from the mass dependence. In particular, for a given quark running in the loop, one obtains a logarithmic dependence on its squared mass, m_i^2. This implies that

$$\Pi^{gg} \supset c\sum_i \log(m_i^2), \tag{8}$$

where c is some constant and the sum is over t, t_1', t_2'. Now in the case under consideration all of the squared masses m_i^2 are the eigenvalues of the matrix $m_f^u m_f^{u\dagger}$ (as given in Appendix A). Since $\sum_i \log(m_i^2) = \log(\Pi_i m_i^2) = \log[\det(m_f^u m_f^{u\dagger})]$ and $\det(m_f^u m_f^{u\dagger}) = \det^2(m_f^u)$, the relevant terms in Π^{gg} are given by

$$\Pi^{gg} \supset c\sum_i \log(m_i^2) = c\log[\det^2(m_f^u)]. \tag{9}$$

Taking the partial derivative,

$$A_{gg\to h} \propto \frac{\partial[\log(\det^2 m_f^u)]}{\partial v} = \frac{1}{\det^2 m_f^u}\frac{\partial \det^2 m_f^u}{\partial v}. \tag{10}$$

In the special case $\bar{y}_{44} = 0$, we have $\det(m_f^u) = v(y_{33}\mu_4^2 \sin\beta)$, which (taking $\sin\beta \approx 1$) is the same as in the SM aside from the factor of μ_4^2, which cancels in the amplitude. Thus $A_{gg\to h} \propto 2/v$, with no dependence on the y_{ij} Yukawas or the vectorlike mass parameter μ_4, and there is no change from the well-known approximate SM amplitude. We ignore contributions from the scalars, as these are suppressed. We note in passing that this expression has the right mass dimension for the g^* multiplying the dimension-five operator in $\mathcal{L}_0$.

B. V_{tb}^{CKM}

The addition of the vectorlike fourth generation will affect both the weak charged currents (CC) and the weak neutral currents (NC) at tree level. In particular, the $W^\pm$ gauge bosons now couple to both left-handed and right-handed particles. Furthermore, including mixing with the top sector will enrich the flavor structure of the model and induce flavor changing neutral currents (FCNCs) in the mass-eigenstate basis. These FCNCs only involve third and fourth generation particles and are therefore fairly unconstrained. In Appendix B we derive the triple and quartic gauge boson interaction terms with the quarks and squarks, as well as the interaction terms between the Higgs h_o and quarks.

The rotation from gauge to mass eigenstates leads to generalized Cabbibo-Kobayashi-Maskawa (CKM) matrices between the third generation, fourth generation, and its mirror generation (which can be viewed as a "fifth" generation), which we denote by K_α^{ab} for quarks, and $\tilde{K}_\alpha^{ab}$ for squarks, with $a, b = u, \bar{u}, d, \bar{d}$ and $\alpha = L, R$. These matrices will be present in every interaction term. Furthermore, they are not square matrices like in the MSSM because there are more up-type quarks than down-type quarks.

The generalized CKM matrix K_L^{ud} is a rectangular (2×3) matrix (see Appendix B for more details) in the mass basis (t, t_1', t_2') for the (four-component) up-type quarks and (b, b') for the down-type quarks. This matrix, being rectangular, is not unitary but satisfies the following equation:

$$\begin{aligned} K_L^{ud}(K_L^{ud})^\dagger + K_L^{\bar{u}\,\bar{u}}(K_L^{\bar{u}\,\bar{u}})^\dagger &= (V_L^{u\dagger} D_L^{ud} V_L^d)(V_L^{u\dagger} D_L^{ud} V_L^d)^\dagger \\ &\quad + (V_L^{u\dagger} S_L^{\bar{u}\,\bar{u}\,\dagger} V_L^u)(V_L^{u\dagger} S_L^{\bar{u}\,\bar{u}\,\dagger} V_L^u)^\dagger \\ &= V_L^{u\dagger}(D_L^{ud} + S_L^{\bar{u}\,\bar{u}})V_L^u \\ &= 1_{3\times 3} \end{aligned}$$

where we have used the unitarity of the mixing matrices V_L^u and V_L^d, and the fact that $D_L^{ud}(D_L^{ud})^\dagger = D_L^{uu}$, $(S_L^{uu})^\dagger S_L^{uu} = S_L^{\bar{u}\,\bar{u}}$ and $D_L^{uu} + S_L^{\bar{u}\,\bar{u}} = 1_{3\times 3}$ (see Appendix C for the explicit form of these matrices).

The $(K_L^{ud})_{11}$ entry predicted by our model should lie within the margin of error of the measured value of V_{tb}^{CKM} [defined as the (3,3) entry of the (3×3) matrix corresponding to the SM CKM matrix V^{CKM}]. As usual, we neglect the mixing between the first two generations and the higher generations. When unitarity of the SM V^{CKM} is not assumed, V_{tb}^{CKM} was recently measured by CMS [50] to be $|V_{tb}^{\mathrm{CKM}}| = 1.14 \pm 0.22$. We therefore require $0.92 < (K_L^{ud})_{11} < 1.36$. After scanning over a large region of our relevant parameter space, we conclude that this restriction is always satisfied. Therefore, the constraints from the measured value of V_{tb}^{CKM} are negligible. This is in agreement with the statements in [46].

C. Mass bounds from LHC direct searches

LHC direct searches are the most obvious source of constraints on the masses of the new vectorlike quarks. The branching ratios of the new quarks depend on the relative size of the relevant Yukawa, W and Z couplings. Until fairly recently, many searches assumed 100% branching ratio through one channel, particularly the Wb decay, and therefore had a large degree of model dependence. However, unlike these searches, ATLAS and CMS now can exclude vectorlike quarks in a model independent way by considering general branching ratio scenarios in their data analysis.

At the LHC, the t' (or b') can be either pair produced or singly produced. Typically, the pair produced initial state has a large cross section; however, as shown in [47] it is possible that single production of the heavy quark via the exchange of a t-channel W has a larger cross

TABLE II. Possible event topologies that could arise at the LHC with initial states involving only one single t' or b'. f denotes any fermion, $(f = q, l)$.

Initial	Intermediate	Final	Initial	Intermediate	Final
t'	ht	$bbWb$	b'	hb	bbb
t'	Zt	$ffWb$	b'	Zb	ffb
t'	Wb	Wb	b'	Wt	WWb
$t't$	htt	$bbWbWb$	$b'b$	hb	$bbbb$
$t't$	Ztt	$ffWbWb$	$b'b$	Zb	$ffbb$
$t't$	Wbt	$WbWb$	$b'b$	Wtb	$WWbb$
$t'bj$	$htbj$	$bbWbbj$	$b'tj$	$hbWbj$	$bbbWbj$
$t'bj$	$Ztbj$	$ffWbbj$	$b'tj$	$ZbWbj$	$ffbWbj$
$t'bj$	$Wbbj$	$Wbbj$	$b'tj$	$WtWbj$	$WWbWbj$

TABLE III. Possible event topologies that could arise at the LHC with initial states involving a pair produced t' or b'. f denotes any fermion, $(f = q, l)$.

Initial	Intermediate	Final	Initial	Intermediate	Final
$t't'$	$htht$	$bbWbbbWb$	$b'b'$	$hbhb$	$bbbbbb$
$t't'$	$htZt$	$bbWbffWb$	$b'b'$	$hbZb$	$bbbffb$
$t't'$	$htWb$	$bbWbWb$	$b'b'$	$hbWt$	$bbWWb$
$t't'$	$ZtZt$	$ffWbffWb$	$b'b'$	$ZbZb$	$ffbffb$
$t't'$	$ZtWb$	$ffWbWb$	$b'b'$	$ZbWt$	$ffbWWb$
$t't'$	$WbWb$	$WbWb$	$b'b'$	$WtWt$	$WWbWWb$

section than $t't'$. This opens new decay chains such as $t'bj \to htbj \to bbWbbj$. In Tables II and III we list possible event topologies that could arise at the LHC. For the final states, we see that there may be as many as six b jets, or if the Higgs decays via the less common WW^* channel then there may be as many as six W bosons. Finally, we note that $t'bj \to Wbbj$ and $t't' \to WbWb$ present two of the best routes to discovery since m_{Wb} would reconstruct to $m_{t'}$ and the signals are relatively clean.

The most recent search done by CMS is the first search to consider all three final states, and puts the most stringent constraints to date on the existence of a heavy vectorlike top quark. Assuming that the heavy vectorlike top quark decays exclusively into bW, tZ, and tH, CMS has set lower limits for its mass between 687 and 782 GeV for all possible branching fractions into these three final states assuming strong production. Their results are summarized in Fig. 6 (taken from [48]).

For ATLAS, the high multiplicity of jets has recently been used in the search for vectorlike quarks, yielding the mass bound on the t' consistent with CMS [51]. Therefore, requiring the vectorlike mass parameter $\mu_4 \gtrsim 700$ ensures that the physical masses of the new heavy quarks are above the lower bounds excluded by the LHC.

D. Electroweak precision observables

We now study the total contribution of the new generation to the electroweak oblique parameters S and T. In Appendix B, we work out the interaction terms between the new particles and the electroweak gauge bosons in the mass basis Lagrangian, as these are needed to derive the necessary Feynman rules to calculate the self-energy loops in the definitions of S and T. The relevant interaction terms are of the form Wff, Zff, Aff and for quarks, and $W\tilde{f}\,\tilde{f}$, $Z\tilde{f}\,\tilde{f}$, $A\tilde{f}\,\tilde{f}$, $WW\tilde{f}\,\tilde{f}$, $ZZ\tilde{f}\,\tilde{f}$, $AA\tilde{f}\,\tilde{f}$ and $ZA\tilde{f}\,\tilde{f}$ for squarks. In Appendix E we calculate the contributions to the oblique parameters from both fermions $(T_f,\ S_f)$ and scalars $(T_s,\ S_s)$. We note that in the full decoupling limit, $\mu_4 \to \infty$ and $y_{ij} \to 0$, we recover SM values.

To get the total contribution of the new sector, we define $T_{\text{new}} = T_f + T_s - T_{\text{SM}}$ and $S_{\text{new}} = S_f + S_s - S_{\text{SM}}$. The values $T_{\text{SM}} \approx 1.22$ and $S_{\text{SM}} \approx -0.08$ were calculated to account for the top sector alone. In general, we find that $T_s \ll T_f$ and $S_f \approx S_s$.

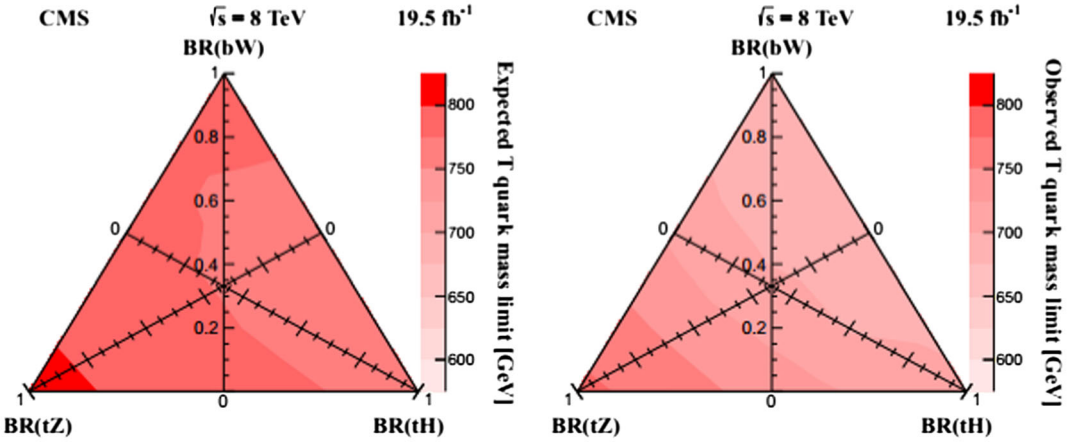

FIG. 6 (color online). Present status of heavy vectorlike top searches with 19.5 fb^{-1} of 8 TeV data with the CMS detector (figure taken from [48]). A branching-fraction triangle is shown with expected (left) and observed 95% C.L. (right) on the mass. Every point in the triangle corresponds to a specific set of branching-fraction values subject to the constraint that all three add up to 1.

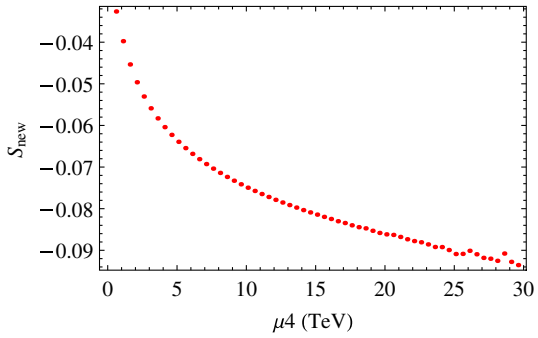

FIG. 7 (color online). S_{new} versus μ_4 for $y_{34} = 0.6$ and $y_{44} = y_{43} = 0$. S_{new} remains small as $\mu_4 \to \infty$.

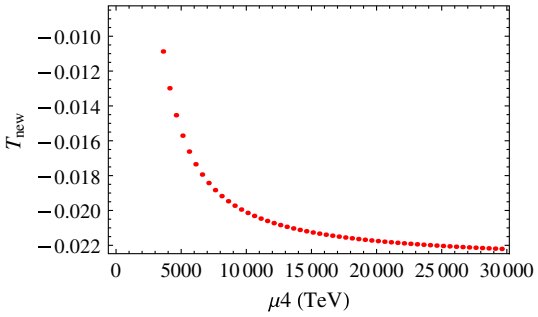

FIG. 8 (color online). T_{new} versus μ_4 for $y_{34} = 0.6$ and $y_{44} = y_{43} = 0$. T_{new} remains small as $\mu_4 \to \infty$.

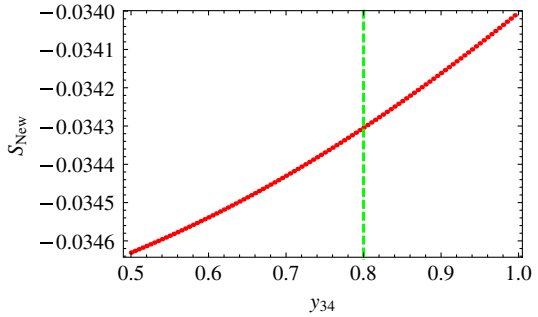

FIG. 9 (color online). S_{new} versus y_{34} for the benchmark scenario $y_{34} \gg y_{44}, y_{43}$, $\mu_4 = 900$ GeV, $A = \Delta m = 800$ GeV. S_{new} remains small in this region. As y_{34} increases from 0.5 to 1, S_{new} increases by a negligible amount of the order of 10^{-4}. The region $y_{34} \gtrsim 0.8$ to the right of the dashed line is disfavored by EWPM due to the T parameter (see Fig. 10).

The μ_4 dependences of S_{new} and T_{new} are shown in Figs. 7 and 8, respectively, for the benchmark scenario $y_{34} = 0.6$ and $y_{44} = y_{43} = 0$ with the Yukawa values kept fixed. As a sanity check, we see that for a large range of μ_4, the values of S and T remain very small.

The dependences of S_{new} and T_{new} on the mixing Yukawa couplings are shown in Figs. 9 and 10, respectively, for the benchmark scenario $y_{34} \gg y_{44}, y_{43}$ with $\mu_4 =$ 900 GeV kept fixed and $A = \Delta m = 800$ GeV. As y_{34} increases from 0.5 to 1, S_{new} increases by a negligible amount of the order of 10^{-4}. However, T_{new} increases by $\sim$0.25. For $T \gtrsim 0.15$, there is tension with the EWPM fit (as can be seen in Fig. 11) and therefore the maximum allowed value for y_{34} in this case is $\sim$0.8.

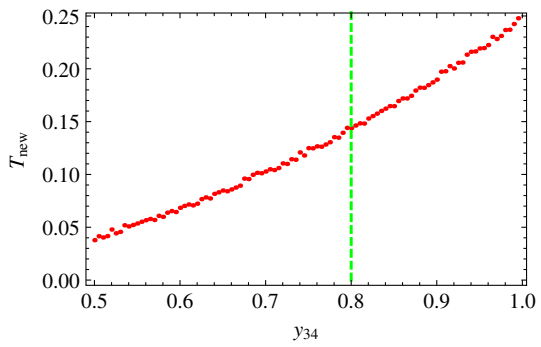

FIG. 10 (color online). T_{new} versus y_{34} for the benchmark scenario $y_{34} \gg y_{44}, y_{43}$, $\mu_4 = 900$ GeV, $A = \Delta m = 800$ GeV. As y_{34} increases from 0.5 to 1, T_{new} increases from $\sim$0.05 to $\sim$0.25. The region $y_{34} \gtrsim 0.8$ to the right of the dashed line is disfavored by EWPM as can be seen in Fig. 11.

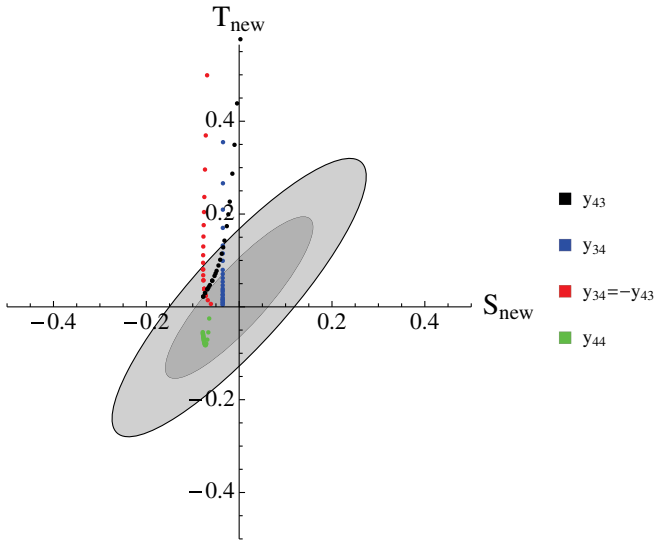

FIG. 11 (color online). We calculate S_{new} and T_{new} for each of the benchmark scenarios: $y_{34} \gg y_{43}, y_{44}$; $y_{43} \gg y_{34}, y_{44}$; and $y_{34} = -y_{43} \gg y_{44}$. Within each scenario $\mu_4 = 900$ GeV, $A = 600$ GeV, and we vary Δm from 300 to 1500 GeV. Each of these points satisfies current mass bounds (see Sec. IV C) and gives a Higgs mass $m_h = 125.5 \pm .5$ GeV while yielding new quarks discoverable at the LHC. The points corresponding to very low Δm and larger Yukawas lie farthest from the best fit, with the agreement improving as Δm grows and the Yukawas decrease. For many of these points the net effect from the new sector falls within the 95% or 68% confidence limits on the electroweak observables. The experimental best fit corresponds to the center of the ellipses, at (0.00,0.02) [52]. The light (dark) grey ellipse denotes the 95% (65%) C.L. on the EW observables. The origin is defined to be the standard model prediction with a 125 GeV Higgs. In concert with the results of Sec. III B, precision electroweak observables permit sufficiently large Yukawa mixing to obtain a Higgs mass $\sim$125 GeV with soft terms below a TeV.

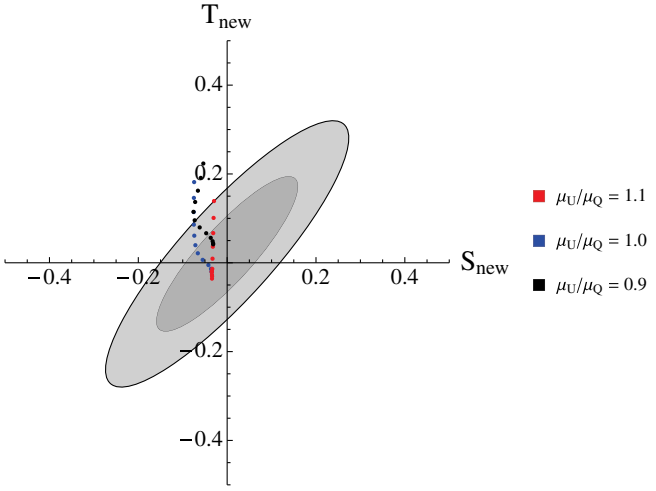

FIG. 12 (color online). We plot the $S_{\rm new}, T_{\rm new}$ for ratios $\mu_U/\mu_Q = 0.9, 1.0, 1.1$, and Yukawa values $y_{34} = -y_{43}$ ranging from 0.01 to 0.56 in steps of 0.05. Each of these points satisfies current mass bounds (see Sec. IV C) and gives a Higgs mass $m_h = 125.5 \pm .5$ GeV while yielding new quarks discoverable at the LHC. The points corresponding to very low Δm and larger Yukawas lie farthest from the best fit, with the agreement improving as Δm grows and the Yukawas decrease. For many of these points the net effect from the new sector falls within the 95% or 68% confidence limits on the electroweak observables. The experimental best fit corresponds to the center of the ellipses, at (0.00,0.02) [52]. The light (dark) grey ellipse denotes the 95% (65%) C.L. on the EW observables. The origin is defined to be the Standard Model prediction with a 125 GeV Higgs. In concert with the results of Sec. III B, precision electroweak observables permit sufficiently large Yukawa mixing to obtain a Higgs mass ∼125 GeV with soft terms below a TeV.

To get a more general picture, we scanned over a wide range of the parameter space from the new sector consistent with the mass bounds from the LHC (see Sec. IV C). We varied y_{ij}, μ_4, and Δm but kept the A terms fixed at 800 GeV. The results are presented in Fig. 11. We see that $-0.1 \lesssim S_{\rm new} \lesssim 0$, while $T_{\rm new}$ can be positive or negative. The positive contributions of $T_{\rm new}$ can be large enough to be in tension with EWPD. Nevertheless, from Fig. 11 it is clear that with vector masses $\mu_4 \gtrsim 900$ GeV a large set of our parameter space of interest falls within the 95% and 68% confidence limits on the electroweak observables.

Furthermore, while taking $\mu_U/\mu_Q = 1$ is a natural simplification, in general this condition does not hold. Indeed, if the vector masses are taken to be equal at some high SUSY-breaking scale, then differences in the beta functions will result in unequal vector masses at the weak scale. We therefore probed the effect of varying this ratio while keeping the sum of the masses constant. The ratio is less constrained for smaller mixing Yukawas, with $2.3 \gtrsim \mu_U/\mu_Q \gtrsim 0.85$ allowed by EWPM for $y_{34} = -y_{43} = 0.1$ and $\mu_Q + \mu_U = 1800$ GeV, while for large $y_{34} = -y_{43}$ we find $1.2 \gtrsim \mu_U/\mu_Q \gtrsim 0.9$. On the other hand, there are scenarios in which the effects from a nonunity ratio value counteract the effects from large mixing Yukawas. For example, with $\mu_U/\mu_Q = 1.1$ it was found that $y_{34} = -y_{43}$ can be as large as 0.56 and still fall within the 95% confidence limits on EWPD, up from 0.43 for a ratio of 1. Since EWPM give the most significant constraints on the y_{ij}, we see by referring to Fig. 1 that soft masses $\lesssim$800 GeV are then the minimum required for the $y_{34} = -y_{43}$ case, rather than the ∼1000 GeV it requires when the ratio is 1 (the y_{ij} needed to give the desired Higgs mass have negligible dependence on the value of the ratio). In Fig. 12 we plot the $S_{\rm new}, T_{\rm new}$ for ratios $\mu_U/\mu_Q = 0.9, 1.0, 1.1$, and Yukawa values $y_{34} = -y_{43}$ ranging from 0.01 to 0.56 in steps of 0.05.

We conclude that in concert with the results of Sec. III B, precision electroweak observables permit sufficiently large Yukawa mixing to obtain a Higgs mass ∼125 GeV with soft parameters below a TeV while yielding new quarks discoverable at the LHC.

V. CONCLUSIONS

In this paper we studied the effects of sizable mixing Yukawa terms between the top sector and a vectorlike quark generation. We computed the energy scale of the Landau pole induced by the top Yukawa for various scenarios. We also discussed the LHC phenomenology and the consequences of including top mixing effects on final state event topologies.

We found that sizable mixing Yukawa couplings (y_{34} and y_{43}) in the superpotential require an increase of the value of the top Yukawa coupling by at most ∼6% to produce the observed top mass. Since loop corrections to m_h go as $y_{\rm top}^4$, mixing will increase the predicted value of the physical Higgs mass, a point not previously emphasized in the literature. This high sensitivity to the top Yukawa is in contrast with the weaker logarithmic dependence on top squark masses.

The mixing Yukawas necessary to achieve a given Higgs mass are smaller when $|y_{34}| \sim |y_{43}|$ than when one of these couplings dominates the other, and if one allows $\mu_U/\mu_Q \neq 1$ then the lowest soft masses ($\Delta m \sim 750$ GeV) can be accommodated for this case. However, under the restriction $\mu_U/\mu_Q = 1$, the lowest possible value of Δm consistent with EWPM is $\Delta m \sim 800$ GeV, which occurs when $y_{34} \sim 0.8$ and $y_{43} = y_{44} = 0$ (see Fig. 1).

Moreover, mixing can significantly raise the Higgs mass while retaining perturbativity to much higher scales than possible with only the self-coupling y_{44} of the fourth generation (see Fig. 2). For A terms and soft masses around 900 GeV, the top Yukawa Landau pole can be pushed above the GUT scale. For $\mu_Q = \mu_U$, soft masses can be as low as 800 GeV and still generate a Higgs mass of 125 GeV, albeit in parts of parameter space with a Landau pole at $\sim 10^{10}$ GeV. Smaller supersymmetry-breaking

terms suffice if one sacrifices perturbativity at the unification scale by adding fields in a $\mathbf{5}+\bar{\mathbf{5}}$ (see Fig. 5).

We studied the constraints from electroweak precision measurements, the measurements of V_{tb}^{CKM}, Higgs production, and the most recent mass bounds from direct searches for vectorlike quarks at the LHC. We found that the oblique corrections and LHC direct searches give the dominant constraints. With vector masses $\mu_4 \gtrsim 900$ GeV and soft scalar masses $\Delta m \gtrsim 800$ GeV, the net effect from the new sector falls within the 95% confidence limits on the electroweak observables.

We conclude that there is a large parameter space available for a supersymmetric model with a vectorlike fourth generation that passes all tests from previous experimental analyses with sufficiently large Yukawa mixing to obtain a Higgs mass ~125 GeV, while yielding new quarks discoverable at the LHC. These models have a soft SUSY-breaking scale that remains moderate and can therefore address the little hierarchy problem.

Finally, we refer to the Appendixes for details about the particle spectrum, the derivation of the mass matrices in the model and the calculation of the oblique parameters. In addition, we give the explicit form of all of the matrices needed to write the interaction Lagrangian. These include generalized CKM matrices, couplings matrices and projection matrices. We also list the beta functions used in the study of Landau poles and perturbativity, as well as loop functions used in the calculation of the oblique parameters.

ACKNOWLEDGMENTS

We particularly thank D. E. Kaplan, as well as S. Rajendran, both of whom made contributions to this work. We also want to thank C. Brust and M. Walters for useful comments.

APPENDIX A: THE PHYSICAL SPECTRUM AND MASS MATRICES

After the $SU(2)_L \times U(1)_Y$ gauge symmetry is broken, Yukawa terms in the superpotential [Eq. (1)], soft terms, F terms, and D terms lead to the following fermion mass matrices,

$$M_f^u = \begin{pmatrix} 0 & m_f^u \\ m_f^{u\dagger} & 0 \end{pmatrix}, \quad \text{with} \quad m_f^u \equiv \begin{pmatrix} y_{33}v_u & y_{34}v_u & 0 \\ y_{43}v_u & y_{44}v_u & \mu_Q \\ 0 & \mu_U & 0 \end{pmatrix},$$

$$M_f^d \equiv \begin{pmatrix} 0 & m_f^d \\ m_f^{d\dagger} & 0 \end{pmatrix}, \quad \text{with} \quad m_f^d \equiv \begin{pmatrix} m_{\mathrm{bot}} & 0 \\ 0 & \mu_Q \end{pmatrix},$$

and the scalar squared mass matrices,

$$(M_s^u)^2 = (M_f^u)^2 + \begin{pmatrix} Y_{u_3} & 0 & 0 & -y_{33}v_uX_u & -y_{34}v_uX_u & 0 \\ 0 & \mu_Q^2 + Y_{u_4} & 0 & -y_{43}v_uX_u & -y_{44}v_uX_u & B\mu \\ 0 & 0 & \mu_U^2 + Y_{\bar{u}_4} & 0 & B\mu & 0 \\ -y_{33}v_uX_u & -y_{43}v_uX_u & 0 & Y_{u_3^c} & 0 & 0 \\ -y_{34}v_uX_u & -y_{44}v_uX_u & B\mu & 0 & \mu_U^2 + Y_{u_4^c} & 0 \\ 0 & B\mu & 0 & 0 & 0 & \mu_Q^2 + Y_{\bar{u}_4^c} \end{pmatrix},$$

$$(M_s^d)^2 = (M_f^d)^2 + \begin{pmatrix} Y_{d_3} & 0 & -m_{\mathrm{bot}}X_d & 0 \\ 0 & \mu_Q^2 + Y_{d_4} & 0 & B\mu \\ -m_{\mathrm{bot}}X_d & 0 & Y_{d_3^c} & 0 \\ 0 & B\mu & 0 & \mu_Q^2 + Y_{\bar{d}_4^c} \end{pmatrix}.$$

Here, $v_u = v\sin\beta$, with $v \approx 174$ GeV, and $m_{\mathrm{bot}} \approx 4.2$ GeV is the mass of the bottom quark. $X_u = A + \mu\cot\beta$ and $X_d = A + \mu\tan\beta$. Along the diagonal, $Y_q \equiv \Delta m^2 + D_a$, where the D-term contribution is $D_a = (T_a^3 - Q_a\sin^2\theta_w)\cos(2\beta)m_Z^2$ for each quark field a, T^3 is the third component of weak isospin, Q_a is the electric charge, and θ_w is the weak mixing angle. We take all parameters to be real. With the mass matrices defined as above, the relevant mass Lagrangian (after EWSB) in the gauge-eigenstate basis can be written as

$$-\mathcal{L}_m = (f_L^{uT} m_f^u f_R^u + f_L^{dT} m_f^d f_R^d + \text{H.c.}) + \tilde{f}^{u\dagger}(M_s^u)^2 \tilde{f}^u + \tilde{f}^{d\dagger}(M_s^d)^2 \tilde{f}^d \quad \text{(A1)}$$

where the basis is

$$\begin{aligned} f_L^u &= (u_3, u_4, \bar{u}_4)^T \\ f_R^u &= (u_3^c, u_4^c, \bar{u}_4^c)^T \\ f_L^d &= (d_3, d_4)^T \\ f_R^d &= (d_3^c, \bar{d}_4^c)^T \\ \tilde{f}^u &= (\tilde{u}_3, \tilde{u}_4, \tilde{\bar{u}}_4, \tilde{u}_3^c, \tilde{u}_4^c, \tilde{\bar{u}}_4^c)^T \\ \tilde{f}^d &= (\tilde{d}_3, \tilde{d}_4, \tilde{d}_3^c, \tilde{\bar{d}}_4^c)^T. \end{aligned} \quad \text{(A2)}$$

The physical masses of the fermions are obtained by bidiagonalizing the fermion mass matrices using the singular value decomposition:

$$\begin{aligned} m_D^u &= V_L^{u\dagger} m_f^u V_R^u \\ m_D^d &= V_L^{d\dagger} m_f^d V_R^d \end{aligned}$$

where $V_L^{u,d}$ and $V_R^{u,d}$ are unitary matrices and the $m_D^{u,d}$ matrices are diagonal. The diagonal entries of m_f^u (m_f^d) correspond to the physical masses of the top (bottom) and the new non-MSSM quarks $t'_{1,2}$ (b'). Similarly, the scalar squared matrices are diagonalized by the unitary matrices $W^{u,d}$ as

$$\begin{aligned} (\tilde{M}_D^u)^2 &= W^{u\dagger}(M_s^u)^2 W^u \\ (\tilde{M}_D^d)^2 &= W^{d\dagger}(M_s^d)^2 W^d, \end{aligned}$$

where the $(\tilde{M}_D^{u,d})^2$ matrices are diagonal. The positive square roots of $(\tilde{M}_D^u)^2$ [and $(\tilde{M}_D^d)^2$] correspond to the physical masses of the tops squarks (sbottoms) and the new non-MSSM squarks $\tilde{t}_{1,2}$, $\tilde{t}'_{1,2,3,4}$ ($\tilde{b}_{1,2}$, $\tilde{b}'_{1,2}$). To obtain a Lagrangian in the mass-eigenstate basis, we rotate the gauge eigenstates by left-multiplying the vectors $f^{u,d}$ and $\tilde{f}^{u,d}$ in Eq. (A2) by the corresponding mixing matrices $V_{L,R}^{u,d\dagger}$ and $W^{u,d\dagger}$, respectively. We denote the mass-eigenstate basis with a hat, $\hat{f}_{L,R}^{u,d} = V_{L,R}^{u,d\dagger} f_{L,R}^{u,d}$ and $\hat{\tilde{f}}^{u,d} = W^{u,d\dagger}\tilde{f}^{u,d}$. A typical particle spectrum is shown in Table IV for $\mu_4 = 900$ GeV.

TABLE IV. A typical particle spectrum for the three different benchmark scenarios: (1) $y_{34} = -y_{43} = 0.8$ and $y_{44} = 0$; (2) $y_{34} = 0.8$ and $y_{43}, y_{44} = 0$; (3) $y_{44} = 0.8$ and $y_{34}, y_{43} = 0$. The scenario $y_{43} = 0.8$ and $y_{34}, y_{44} = 0$ gives the same masses as scenario (2) and we therefore omit it. We set $A = \Delta m = \mu_4 = 900$ GeV. As we can see, mixing does not change drastically the mass spectrum.

Mass (GeV)	Scenario 1	Scenario 2	Scenario 3
$m_{t'_1}$	909	900	900
$m_{t'_2}$	913	911	900
$m_{b'}$	900	900	900
$\tilde{m}_{\tilde{t}_1}$	814	818	821
$\tilde{m}_{\tilde{t}_2}$	982	991	1000
$\tilde{m}_{\tilde{t}'_1}$	1275	1271	1271
$\tilde{m}_{\tilde{t}'_2}$	1276	1273	1272
$\tilde{m}_{\tilde{t}'_3}$	1287	1275	1273
$\tilde{m}_{\tilde{t}'_4}$	1300	1294	1274
$\tilde{m}_{\tilde{b}_1}$	860	860	860
$\tilde{m}_{\tilde{b}_2}$	940	940	940
$\tilde{m}_{\tilde{b}'_1}$	1271	1271	1271
$\tilde{m}_{\tilde{b}'_2}$	1274	1275	1274

APPENDIX B: THE INTERACTION LAGRANGIAN

The rotation from gauge to mass eigenstates leads to generalized CKM matrices between the third and fourth generation, which we denote by K_α^{ab} for quarks, and $\tilde{K}_\alpha^{ab}$ for squarks, with $a, b = u, \bar{u}, d, \bar{d}$ and $\alpha = L, R$. These matrices will be present in every interaction term. Furthermore, they are not square matrices like in the MSSM because there are more up-type quarks (squarks) than down-type quarks (squarks). Their general form is $K_\alpha^{ab} = V_\alpha^{a\dagger} D_\alpha^{ab} V_\alpha^b$ or $K_\alpha^{ab} = V_\alpha^{a\dagger} S_\alpha^{ab} V_\alpha^b$, and $\tilde{K}_\alpha^{ab} = W^\dagger \tilde{D}_\alpha^{ab} W$ or $\tilde{K}_\alpha^{ab} = W^\dagger \tilde{S}_\alpha^{ab} W$. The projection matrices, D_α^{ab} and $\tilde{D}_\alpha^{ab}$ (S_α^{ab} and $\tilde{S}_\alpha^{ab}$) select the appropriate doublet (singlet) field component of f^a and $\tilde{f}^a$, respectively, before rotating to the mass basis. We note that, in general, $K_\alpha^{aa} = K_\alpha^{ab} K_\alpha^{ab\dagger}$, so we can construct all of the generalized CKM matrices from all the possible products of K_α^{ab} and $K_\alpha^{ab\dagger}$. It is therefore the nonunitarity and off-diagonal entries of K_α^{ab} that leads to FCNCs. K_α^{ab} and $\tilde{K}_\alpha^{ab}$ depend on the flavor and chirality of the particles involved in the interaction, and on the parameters of the model (e.g. μ_4, y_{ij}) which are present in the corresponding mixing matrices V_α^a and W^a.

In Tables V and VI, we give the form of all these generalized CKM matrices and write down the corresponding interaction term coupling the vector bosons $V_\mu = W_\mu, Z_\mu, A_\mu$ to the quarks or squarks, in the mass basis. The matrices D_α^{ab}, $\tilde{D}_\alpha^{ab}$, S_α^{ab} and $\tilde{S}_\alpha^{ab}$ are listed in Appendix C, and the mixing matrices V_α^a and W^a were calculated numerically and depend on the parameters of the model.

As an example, let us write down in matrix form the term in the Lagrangian corresponding to the charged current interaction vertex W^+ff. In terms of the gauge-eigenstate basis vectors $f_L^{u\dagger}$ (a three-dimensional row vector in generation space) and $f_L^{d\dagger}$ (a two-dimensional column vector in generation space), the interaction term needs a 3×2 projection matrix, which we call D_L^{ud}, to couple the

TABLE V. We give the form of all the generalized CKM matrices K_α^{ab} and their corresponding triple interaction term coupling the vector bosons $V_\mu = W_\mu, Z_\mu, A_\mu$ to the quarks in the mass basis [see Eq. (B2)]. Here, $\hat{f}_\alpha^a$ are the quark vectors in Eq. (A2), and $a, b = u, \bar{u}, d, \bar{d}$ and $\alpha = L, R$. The projection matrices D_α^{ab} and S_α^{ab} are listed in Appendix C. The mixing matrices V_α^a were calculated numerically and depend on the parameters of the model.

$V_\mu \hat{f}_\alpha^{a\dagger} K_\alpha^{ab} \bar{\sigma}^\mu \hat{f}_\alpha^b$	K_α^{ab}
$W_\mu^+ \hat{f}_L^{u\dagger} K_L^{ud} \bar{\sigma}^\mu \hat{f}_L^d$	$V_L^{u\dagger} D_L^{ud} V_L^d$
$W_\mu^+ \hat{f}_R^{d\dagger} K_R^{\bar{u}\bar{d}\,\dagger} \bar{\sigma}^\mu \hat{f}_R^u$	$V_R^{u\dagger} D_R^{\bar{u}\bar{d}} V_R^d$
$Z_\mu^0 \hat{f}_L^{u\dagger} K_L^{uu} \bar{\sigma}^\mu \hat{f}_L^u$	$V_L^{u\dagger} D_L^{uu} V_L^u$
$Z_\mu^0 \hat{f}_L^{u\dagger} K_L^{\bar{u}\bar{u}} \bar{\sigma}^\mu \hat{f}_L^u$	$V_L^{u\dagger} S_L^{\bar{u}\bar{u}} V_L^u$
$Z_\mu^0 \hat{f}_R^{u\dagger} K_R^{\bar{u}\bar{u}} \bar{\sigma}^\mu \hat{f}_R^u$	$V_R^{u\dagger} D_R^{\bar{u}\bar{u}} V_R^u$
$Z_\mu^0 \hat{f}_R^{u\dagger} K_R^{uu} \bar{\sigma}^\mu \hat{f}_R^u$	$V_R^{u\dagger} S_R^{uu} V_R^u$
$Z_\mu^0 \hat{f}_L^{d\dagger} K_L^{dd} \bar{\sigma}^\mu \hat{f}_L^d$	$V_L^{d\dagger} D_L^{dd} V_L^d$
$Z_\mu^0 \hat{f}_R^{d\dagger} K_R^{\bar{d}\bar{d}} \bar{\sigma}^\mu \hat{f}_R^d$	$V_R^{d\dagger} D_R^{\bar{d}\bar{d}} V_R^d$
$Z_\mu^0 \hat{f}_R^{d\dagger} K_R^{dd} \bar{\sigma}^\mu \hat{f}_R^d$	$V_R^{d\dagger} S_R^{dd} V_R^d$

left-handed (LH) fields with $T_3 = 1/2$ (u_3^c and u_4^c) in $f_L^{u\dagger}$ to the LH fields with $T_3 = -1/2$ (d_3 and d_4) in f_L^d. This gives a term $\propto W_\mu^+ f_L^{u\dagger} D_L^{ud} \bar{\sigma}^\mu f_L^d$. Similarly, in terms of the gauge-eigenstate basis vectors $f_R^{d\dagger}$ (a two-dimensional row vector in generation space) and f_R^u (a three-dimensional column vector in generation space), the interaction term needs a 2×3 projection matrix, $D_R^{\bar{u}\bar{d}}$, to couple the right-handed (RH) field with $T_3 = 1/2$ ($\bar{d}_4$) in $f_R^{d\dagger}$ to the RH field with $T_3 = -1/2$ ($\bar{u}_4^c$) in f_R^u. This gives a new term $\propto W_\mu^+ f_R^{d\dagger} D_R^{\bar{u}\bar{d}\,\dagger} \bar{\sigma}^\mu f_R^u$ that is not in the MSSM which couples RH fields to the W boson. After rotating to the mass-eigenstate basis and including the couplings, we get

TABLE VI. We give the form of all the generalized CKM matrices $\tilde{K}_\alpha^{ab}$ and their corresponding triple and quartic interaction terms coupling the vector bosons $V_\mu = W_\mu, Z_\mu, A_\mu$ to the squarks in the mass basis [see Eq. (B3)]. Here, $\hat{\tilde{f}}^a$ are the squark vectors in Eq. (A2), and $a, b = u, \bar{u}, d, \bar{d}$ and $\alpha = L, R$. The projection matrices $\tilde{D}_\alpha^{ab}$ and $\tilde{S}_\alpha^{ab}$ are listed in Appendix C. The mixing matrices W^a were calculated numerically and depend on the parameters of the model.

$V_\mu \hat{\tilde{f}}^{a\dagger} \tilde{K}_\alpha^{ab} \overleftrightarrow{\partial^\mu} \hat{\tilde{f}}^b$	$V_\mu V^\mu \hat{\tilde{f}}^{a\dagger} \tilde{K}_\alpha^{ab} \hat{\tilde{f}}^b$	$\tilde{K}_\alpha^{ab}$
$W_\mu^+ \hat{\tilde{f}}^{u\dagger} \tilde{K}_L^{ud} \overleftrightarrow{\partial^\mu} \hat{\tilde{f}}^d$	$W_\mu^+ W^{\mu+} \hat{\tilde{f}}^{u\dagger} \tilde{K}_L^{ud} \hat{\tilde{f}}^d$	$W^{u\dagger} \tilde{D}_L^{ud} W^d$
$W_\mu^+ \hat{\tilde{f}}^{d\dagger} \tilde{K}_R^{\bar{u}\bar{d}\,\dagger} \overleftrightarrow{\partial^\mu} \hat{\tilde{f}}^u$	$W_\mu^+ W^{\mu+} \hat{\tilde{f}}^{d\dagger} \tilde{K}_R^{\bar{u}\bar{d}\,\dagger} \hat{\tilde{f}}^u$	$W^{u\dagger} \tilde{D}_R^{\bar{u}\bar{d}} W^d$
$Z_\mu^0 \hat{\tilde{f}}^{u\dagger} \tilde{K}_L^{uu} \overleftrightarrow{\partial^\mu} \hat{\tilde{f}}^u$	$Z_\mu^0 Z^{\mu 0} \hat{\tilde{f}}^{u\dagger} \tilde{K}_L^{uu} \hat{\tilde{f}}^u$	$W^{u\dagger} \tilde{D}_L^{uu} W^u$
$Z_\mu^0 \hat{\tilde{f}}^{u\dagger} \tilde{K}_L^{\bar{u}\bar{u}} \overleftrightarrow{\partial^\mu} \hat{\tilde{f}}^u$	$Z_\mu^0 Z^{\mu 0} \hat{\tilde{f}}^{u\dagger} \tilde{K}_L^{\bar{u}\bar{u}} \hat{\tilde{f}}^u$	$W^{u\dagger} \tilde{S}_L^{\bar{u}\bar{u}} W^u$
$Z_\mu^0 \hat{\tilde{f}}^{u\dagger} \tilde{K}_R^{\bar{u}\bar{u}} \overleftrightarrow{\partial^\mu} \hat{\tilde{f}}^u$	$Z_\mu^0 Z^{\mu 0} \hat{\tilde{f}}^{u\dagger} \tilde{K}_R^{\bar{u}\bar{u}} \hat{\tilde{f}}^u$	$W^{u\dagger} \tilde{D}_R^{\bar{u}\bar{u}} W^u$
$Z_\mu^0 \hat{\tilde{f}}^{u\dagger} \tilde{K}_R^{uu} \overleftrightarrow{\partial^\mu} \hat{\tilde{f}}^u$	$Z_\mu^0 Z^{\mu 0} \hat{\tilde{f}}^{u\dagger} \tilde{K}_R^{uu} \hat{\tilde{f}}^u$	$W^{u\dagger} \tilde{S}_R^{uu} W^u$
$Z_\mu^0 \hat{\tilde{f}}^{d\dagger} \tilde{K}_L^{dd} \overleftrightarrow{\partial^\mu} \hat{\tilde{f}}^d$	$Z_\mu^0 Z^{\mu 0} \hat{\tilde{f}}^{d\dagger} \tilde{K}_L^{dd} \hat{\tilde{f}}^d$	$W^{d\dagger} \tilde{D}_L^{dd} W^d$
$Z_\mu^0 \hat{\tilde{f}}^{d\dagger} \tilde{K}_R^{\bar{d}\bar{d}} \overleftrightarrow{\partial^\mu} \hat{\tilde{f}}^d$	$Z_\mu^0 Z^{\mu 0} \hat{\tilde{f}}^{d\dagger} \tilde{K}_R^{\bar{d}\bar{d}} \hat{\tilde{f}}^d$	$W^{d\dagger} \tilde{D}_R^{\bar{d}\bar{d}} W^d$
$Z_\mu^0 \hat{\tilde{f}}^{d\dagger} \tilde{K}_R^{dd} \overleftrightarrow{\partial^\mu} \hat{\tilde{f}}^d$	$Z_\mu^0 Z^{\mu 0} \hat{\tilde{f}}^{d\dagger} \tilde{K}_R^{dd} \hat{\tilde{f}}^d$	$W^{d\dagger} \tilde{S}_R^{dd} W^d$

$$-\mathcal{L}_{W^+ff} = \frac{g}{\sqrt{2}} W_\mu^+ \hat{f}_L^{u\dagger} K_L^{ud} \bar{\sigma}^\mu \hat{f}_L^d + \frac{g}{\sqrt{2}} W_\mu^+ \hat{f}_R^{d\dagger} K_R^{\bar{u}\bar{d}\,\dagger} \bar{\sigma}^\mu \hat{f}_R^u \tag{B1}$$

from which the coupling matrix $G_{ud}^W = \frac{g}{\sqrt{2}} K_L^{ud}$ and $G_{\bar{u}\bar{d}}^W = -\frac{g}{\sqrt{2}} K_R^{\bar{u}\bar{d}}$ can be extracted. We give the explicit form of the coupling matrices in Tables VII, VIII and IX.

Proceeding similarly to the above example, the interaction Lagrangian for gauge bosons, quarks and the Higgs in the mass-eigenstate basis is

$$\begin{aligned}
-\mathcal{L}_f = {} & W_\mu^+ (\hat{f}_L^{u\dagger} G_{ud}^W \bar{\sigma}^\mu \hat{f}_L^d + \hat{f}_R^{d\dagger} G_{\bar{u}\bar{d}}^{W\dagger} \bar{\sigma}^\mu \hat{f}_R^u) + W_\mu^- (\hat{f}_L^{d\dagger} G_{ud}^{W\dagger} \bar{\sigma}^\mu \hat{f}_L^u + \hat{f}_R^{u\dagger} G_{\bar{u}\bar{d}}^W \bar{\sigma}^\mu \hat{f}_R^d) \\
& + Z_\mu^0 (\hat{f}_L^{u\dagger} G_{u_L}^Z \bar{\sigma}^\mu \hat{f}_L^u + \hat{f}_L^{d\dagger} G_{d_L}^Z \bar{\sigma}^\mu \hat{f}_L^d + \hat{f}_R^{u\dagger} G_{u_R}^Z \bar{\sigma}^\mu \hat{f}_R^u + \hat{f}_R^{d\dagger} G_{d_R}^Z \bar{\sigma}^\mu \hat{f}_R^d) \\
& + A_\mu (\hat{f}_L^{u\dagger} G_{u_L}^A \bar{\sigma}^\mu \hat{f}_L^u + \hat{f}_L^{d\dagger} G_{d_L}^A \bar{\sigma}^\mu \hat{f}_L^d + \hat{f}_R^{u\dagger} G_{u_R}^A \bar{\sigma}^\mu \hat{f}_R^u + \hat{f}_R^{d\dagger} G_{d_R}^A \bar{\sigma}^\mu \hat{f}_R^d) \\
& + (h_o \hat{f}_L^{uT} Y^{u\bar{u}} \hat{f}_R^u + h_o \hat{f}_L^{dT} Y^{d\bar{d}} \hat{f}_R^d + \text{H.c.})
\end{aligned} \tag{B2}$$

where $Y^{u\bar{u}} = V_L^{u\dagger} y^{u\bar{u}} V_R^u$ and $Y^{d\bar{d}} = V_L^{d\dagger} y^{d\bar{d}} V_R^d$, with y^{ab} defined as in Appendix C, are the matrices coupling the scalar Higgs to the quarks. Similarly, the interaction Lagrangian for gauge bosons and squarks in the mass-eigenstate basis is

$$\begin{aligned}
-\mathcal{L}_{\tilde{f}} = {} & W_\mu^+ \left(\hat{\tilde{f}}^{u\dagger} \tilde{G}_{ud}^W \overleftrightarrow{\partial^\mu} \hat{\tilde{f}}^d + \hat{\tilde{f}}^{d\dagger} \tilde{G}_{\bar{u}\bar{d}}^{W\dagger} \overleftrightarrow{\partial^\mu} \hat{\tilde{f}}^u \right) + W_\mu^- \left(\hat{\tilde{f}}^{d\dagger} \tilde{G}_{ud}^{W\dagger} \overleftrightarrow{\partial^\mu} \hat{\tilde{f}}^u + \hat{\tilde{f}}^{u\dagger} \tilde{G}_{\bar{u}\bar{d}}^W \overleftrightarrow{\partial^\mu} \hat{\tilde{f}}^d \right) \\
& + Z_\mu^0 \left(\hat{\tilde{f}}^{u\dagger} \tilde{G}_u^Z \overleftrightarrow{\partial^\mu} \hat{\tilde{f}}^u + \hat{\tilde{f}}^{d\dagger} \tilde{G}_d^Z \overleftrightarrow{\partial^\mu} \hat{\tilde{f}}^d \right) + A_\mu \left(\hat{\tilde{f}}^{u\dagger} \tilde{G}_u^A \overleftrightarrow{\partial^\mu} \hat{\tilde{f}}^u + \hat{\tilde{f}}^{d\dagger} \tilde{G}_d^A \overleftrightarrow{\partial^\mu} \hat{\tilde{f}}^d \right) \\
& + W_\mu^+ W^{-\mu} \left(\hat{\tilde{f}}^{u\dagger} \tilde{G}_u^{WW} \hat{\tilde{f}}^u + \hat{\tilde{f}}^{d\dagger} \tilde{G}_d^{WW} \hat{\tilde{f}}^d \right) + Z_\mu^0 Z^{0\mu} \left(\hat{\tilde{f}}^{u\dagger} \tilde{G}_u^{ZZ} \hat{\tilde{f}}^u + \hat{\tilde{f}}^{d\dagger} \tilde{G}_d^{ZZ} \hat{\tilde{f}}^d \right) \\
& + Z_\mu^0 A^\mu \left(\hat{\tilde{f}}^{u\dagger} \tilde{G}_u^{ZA} \hat{\tilde{f}}^u + \hat{\tilde{f}}^{d\dagger} \tilde{G}_d^{ZA} \hat{\tilde{f}}^d \right) + A_\mu A^\mu \left(\hat{\tilde{f}}^{u\dagger} \tilde{G}_u^{AA} \hat{\tilde{f}}^u + \hat{\tilde{f}}^{d\dagger} \tilde{G}_d^{AA} \hat{\tilde{f}}^d \right).
\end{aligned} \tag{B3}$$

TABLE VII. The coupling matrices at the triple vertex between squarks and gauge bosons. We define $g^Z_{(T^3,Q)} = \frac{g}{\cos\theta_W}(T^3 - Q\sin^2\theta_W)$, $g^A_Q = Qe$.

Coupling matrix	Explicit form
G^W_{ud}	$\frac{g}{\sqrt{2}}K^{ud}_L$
$G^Z_{u_L}$	$g^Z_{(\frac{1}{2},\frac{2}{3})}K^{uu}_L + g^Z_{(0,\frac{2}{3})}K^{\bar{u}\bar{u}}_L$
$G^Z_{d_L}$	$g^Z_{(-\frac{1}{2},-\frac{1}{3})}K^{dd}_L$
$G^A_{u_L}$	$g^A_{\frac{2}{3}}[K^{uu}_L + K^{\bar{u}\bar{u}}_L]$
$G^A_{d_L}$	$g^A_{-\frac{1}{3}}K^{dd}_L$
$G^W_{\bar{u}\bar{d}}$	$-\frac{g}{\sqrt{2}}K^{\bar{u}\bar{d}}_R$
$G^Z_{u_R}$	$g^Z_{(0,-\frac{2}{3})}K^{uu}_R + g^Z_{(-\frac{1}{2},-\frac{2}{3})}K^{\bar{u}\bar{u}}_R$
$G^Z_{d_R}$	$g^Z_{(0,\frac{1}{3})}K^{dd}_R + g^Z_{(\frac{1}{2},\frac{1}{3})}K^{\bar{d}\bar{d}}_R$
$G^A_{u_R}$	$g^A_{\frac{2}{3}}[K^{uu}_R + K^{\bar{u}\bar{u}}_R]$
$G^A_{d_R}$	$g^A_{-\frac{1}{3}}K^{dd}_R$

TABLE VIII. The coupling matrices at the triple vertex between quarks and gauge bosons. We define $g^Z_{(T^3,Q)} = \frac{g}{\cos\theta_W}(T^3 - Q\sin^2\theta_W)$, $g^A_Q = Qe$.

Coupling matrix	Explicit form
$\tilde{G}^W_{ud}$	$\frac{g}{\sqrt{2}}\tilde{K}^{ud}_L$
$\tilde{G}^Z_u$	$g^Z_{(\frac{1}{2},\frac{2}{3})}\tilde{K}^{uu}_L + g^Z_{(0,\frac{2}{3})}\tilde{K}^{\bar{u}\bar{u}}_L + g^Z_{(0,-\frac{2}{3})}\tilde{K}^{uu}_R + g^Z_{(-\frac{1}{2},-\frac{2}{3})}\tilde{K}^{\bar{u}\bar{u}}_R$
$\tilde{G}^A_u$	$g^A_{\frac{2}{3}}\tilde{K}^{uu}_L + g^A_{\frac{2}{3}}\tilde{K}^{\bar{u}\bar{u}}_L + g^A_{-\frac{2}{3}}\tilde{K}^{uu}_R + g^A_{-\frac{2}{3}}\tilde{K}^{\bar{u}\bar{u}}_R$
$\tilde{G}^W_{\bar{u}\bar{d}}$	$-\frac{g}{\sqrt{2}}\tilde{K}^{\bar{u}\bar{d}}_R$
$\tilde{G}^Z_d$	$g^Z_{(-\frac{1}{2},-\frac{1}{3})}\tilde{K}^{dd}_L + g^Z_{(0,\frac{1}{3})}\tilde{K}^{dd}_R + g^Z_{(\frac{1}{2},\frac{1}{3})}\tilde{K}^{\bar{d}\bar{d}}_R$
$\tilde{G}^A_d$	$g^A_{-\frac{1}{3}}\tilde{K}^{dd}_L + g^A_{\frac{1}{3}}\tilde{K}^{dd}_R + g^A_{\frac{1}{3}}\tilde{K}^{\bar{d}\bar{d}}_R$

APPENDIX C: PROJECTION MATRICES

Below, we write down explicitly all of the projection matrices D^{ab}_α, S^{ab}_α, $\tilde{D}^{ab}_\alpha$ and $\tilde{S}^{ab}_\alpha$ used in the construction of the generalized CKM matrices (see Appendix B). It follows that only D^{ud}_L and $D^{\bar{u}\bar{d}}_R$ (and $\tilde{D}^{ud}_L$ and $\tilde{D}^{\bar{u}\bar{d}}_R$) are independent, since all of the other matrices can be obtained from their products. For example, $D^{ud}_L(D^{ud}_L)^\dagger = D^{uu}_L$, $(S^{uu}_L)^\dagger S^{uu}_L = S^{\bar{u}\bar{u}}_L$. It also follows that $D^{uu}_L + S^{\bar{u}\bar{u}}_L = 1_{3\times 3}$. For completeness, we also include the matrices $y^{ab} \subset Y^{ab}$ present in the interaction term coupling the Higgs scalar particle to all third and fourth generation quarks (see (B2).

1. Quark sector

$$D^{ud}_L = \begin{pmatrix} 1 & 0 \\ 0 & 1 \\ 0 & 0 \end{pmatrix}. \quad \text{Couples } \left(T_3 = \frac{-1}{2}\right) u^\dagger_3, \qquad u^\dagger_4 \in f^{u\dagger}_L \quad \text{to } \left(T_3 = \frac{1}{2}\right) d_3, \qquad d_4 \in f^d_L.$$

$$D^{\bar{u}\bar{d}}_R = \begin{pmatrix} 0 & 0 \\ 0 & 0 \\ 0 & 1 \end{pmatrix}. \quad \text{Couples } \left(T_3 = \frac{-1}{2}\right) \bar{d}^{c\dagger}_4 \in f^{d\dagger}_R \quad \text{to } \left(T_3 = \frac{1}{2}\right) \bar{u}^c_4 \in f^u_R.$$

TABLE IX. The coupling matrices at the quartic vertex between squarks and gauge bosons. We define $g^Z_{(T^3,Q)} = \frac{g}{\cos\theta_W}(T^3 - Q\sin^2\theta_W)$, $g^A_Q = Qe$.

Coupling Matrix	Explicit Form
$\tilde{G}^{WW}_u$	$\frac{g^2}{2}[\tilde{K}^{uu}_L + \tilde{K}^{\bar{u}\bar{u}}_R]$
$\tilde{G}^{WW}_d$	$\frac{g^2}{2}[\tilde{K}^{dd}_L + \tilde{K}^{\bar{d}\bar{d}}_R]$
$\tilde{G}^{ZZ}_u$	$(g^Z_{(\frac{1}{2},\frac{2}{3})})^2\tilde{K}^{uu}_L + (g^Z_{(0,\frac{2}{3})})^2\tilde{K}^{\bar{u}\bar{u}}_L + (g^Z_{(0,-\frac{2}{3})})^2\tilde{K}^{uu}_R + (g^Z_{(-\frac{1}{2},-\frac{2}{3})})^2\tilde{K}^{\bar{u}\bar{u}}_R$
$\tilde{G}^{ZZ}_d$	$(g^Z_{(-\frac{1}{2},-\frac{1}{3})})^2\tilde{K}^{dd}_L + (g^Z_{(0,\frac{1}{3})})^2\tilde{K}^{dd}_R + (g^Z_{(\frac{1}{2},\frac{1}{3})})^2\tilde{K}^{\bar{d}\bar{d}}_R$
$\tilde{G}^{ZA}_u$	$2[g^A_{\frac{2}{3}}g^Z_{(\frac{1}{2},\frac{2}{3})}\tilde{K}^{uu}_L + g^A_{-\frac{2}{3}}g^Z_{(0,\frac{2}{3})}\tilde{K}^{\bar{u}\bar{u}}_L + g^A_{\frac{2}{3}}g^Z_{(0,-\frac{2}{3})}\tilde{K}^{uu}_R + g^A_{-\frac{2}{3}}g^Z_{(-\frac{1}{2},-\frac{2}{3})}\tilde{K}^{\bar{u}\bar{u}}_R]$
$\tilde{G}^{ZA}_d$	$2[g^A_{-\frac{1}{3}}g^Z_{(-\frac{1}{2},-\frac{1}{3})}\tilde{K}^{dd}_L + g^A_{-\frac{1}{3}}g^Z_{(0,\frac{1}{3})}\tilde{K}^{dd}_R + g^A_{\frac{1}{3}}g^Z_{(\frac{1}{2},\frac{1}{3})}\tilde{K}^{\bar{d}\bar{d}}_R]$
$\tilde{G}^{AA}_u$	$2(g^A_{\frac{2}{3}})^2[\tilde{K}^{uu}_L + \tilde{K}^{\bar{u}\bar{u}}_L + \tilde{K}^{uu}_R + \tilde{K}^{\bar{u}\bar{u}}_R]$
$\tilde{G}^{AA}_d$	$2(g^A_{\frac{1}{3}})^2[\tilde{K}^{dd}_L + \tilde{K}^{dd}_R + \tilde{K}^{\bar{d}\bar{d}}_R]$

From the two matrices above, we can construct

(i) $D_L^{uu} = \mathrm{Diag}(1,1,0)$. Couples $(T_3 = \frac{-1}{2})$ $u_3^\dagger, u_4^\dagger \in f_L^{u\dagger}$ to $(T_3 = \frac{1}{2})$ $u_3, u_4 \in f_L^u$.
(ii) $S_L^{\bar{u}\,\bar{u}} = \mathrm{Diag}(0,0,1)$. Couples $(T_3 = 0)$ $\bar{u}_4^c \in f_L^{u\dagger}$ to $(T_3 = 0)$ $\bar{u}_4 \in f_L^u$.
(iii) $S_R^{uu} = \mathrm{Diag}(1,1,0)$. Couples $(T_3 = 0)$ $u_3^{c\dagger}, u_4^{c\dagger} \in f_R^{u\dagger}$ to $(T_3 = 0)$ $u_3^c, u_4^c \in f_R^u$.
(iv) $D_R^{\bar{u}\,\bar{u}} = \mathrm{Diag}(0,0,1)$. Couples $(T_3 = \frac{1}{2})$ $\bar{u}_4^{c\dagger} \in f_R^{u\dagger}$ to $(T_3 = \frac{-1}{2})$ $\bar{u}_4^c \in f_R^u$.
(v) $D_L^{dd} = \mathrm{Diag}(1,1)$. Couples $(T_3 = \frac{1}{2})$ $d_3^\dagger, d_4^\dagger \in f_L^{d\dagger}$ to $(T_3 = \frac{-1}{2})$ $d_3, d_4 \in f_L^d$.
(vi) $S_R^{dd} = \mathrm{Diag}(1,0)$. Couples $(T_3 = 0)$ $d_3^{c\dagger} \in f_R^{d\dagger}$ to $(T_3 = 0)$ $d_3^c \in f_R^d$.
(vii) $D_R^{\bar{d}\,\bar{d}} = \mathrm{Diag}(0,1)$. Couples $(T_3 = \frac{-1}{2})$ $\bar{d}_4^{c\dagger} \in f_R^{u\dagger}$ to $(T_3 = \frac{1}{2})$ $\bar{d}_4^c \in f_R^d$.

2. Squark sector

$$\tilde{D}_L^{ud} = \begin{pmatrix} 1&0&0&0\\ 0&1&0&0\\ 0&0&0&0\\ 0&0&0&0\\ 0&0&0&0\\ 0&0&0&0 \end{pmatrix}. \quad \mathrm{Couples}\left(T_3 = \frac{-1}{2}\right)\tilde{u}_3^*, \quad \tilde{u}_4^* \in \tilde{f}^{u\dagger} \quad \text{to} \left(T_3 = \frac{1}{2}\right)\tilde{d}_3, \quad \tilde{d}_4 \in \tilde{f}^d.$$

$$\tilde{D}_R^{\bar{u}\,\bar{d}} = \begin{pmatrix} 0&0&0&0\\ 0&0&0&0\\ 0&0&0&0\\ 0&0&0&0\\ 0&0&0&0\\ 0&0&0&1 \end{pmatrix}. \quad \mathrm{Couples}\left(T_3 = \frac{-1}{2}\right)\tilde{\bar{d}}_4^{c*} \in \tilde{f}^{d\dagger} \quad \text{to} \left(T_3 = \frac{1}{2}\right)\tilde{\bar{u}}_4^c \in \tilde{f}^u.$$

From the two matrices above, we can construct

(i) $\tilde{D}_L^{uu} = \mathrm{Diag}(1,1,0,0,0,0)$. Couples $(T_3 = \frac{-1}{2})$ $\tilde{u}_3^*, \tilde{u}_4^* \in \tilde{f}^{u\dagger}$ to $(T_3 = \frac{1}{2})$ $u_3, u_4 \in \tilde{f}^u$.
(ii) $\tilde{S}_L^{\bar{u}\,\bar{u}} = \mathrm{Diag}(0,0,1,0,0,0)$. Couples $(T_3 = 0)$ $\tilde{\bar{u}}_4^c \in \tilde{f}^{u\dagger}$ to $(T_3 = 0)$ $\bar{u}_4 \in \tilde{f}^u$.
(iii) $\tilde{S}_R^{uu} = \mathrm{Diag}(0,0,0,1,1,0)$. Couples $(T_3 = 0)$ $\tilde{u}_3^{c*}, \tilde{u}_4^{c*} \in \tilde{f}^{u\dagger}$ to $(T_3 = 0)$ $\tilde{u}_3^c, \tilde{u}_4^c \in \tilde{f}^u$.
(iv) $\tilde{D}_R^{\bar{u}\,\bar{u}} = \mathrm{Diag}(0,0,0,0,0,1)$. Couples $(T_3 = \frac{1}{2})$ $\tilde{\bar{u}}_4^{c*} \in \tilde{f}^{u\dagger}$ to $(T_3 = \frac{-1}{2})$ $\tilde{\bar{u}}_4^c \in \tilde{f}^u$.
(v) $\tilde{D}_L^{dd} = \mathrm{Diag}(1,1,0,0)$. Couples $(T_3 = \frac{1}{2})$ $\tilde{d}_3^*, \tilde{d}_4^* \in \tilde{f}^{d\dagger}$ to $(T_3 = \frac{-1}{2})$ $\tilde{d}_3, \tilde{d}_4 \in \tilde{f}^d$.
(vi) $\tilde{S}_R^{dd} = \mathrm{Diag}(0,0,1,0)$. Couples $(T_3 = 0)$ $\tilde{d}_3^{c*} \in \tilde{f}^{d\dagger}$ to $(T_3 = 0)$ $\tilde{\bar{d}}_3^c \in \tilde{f}^d$.
(vii) $\tilde{D}_R^{\bar{d}\,\bar{d}} = \mathrm{Diag}(0,0,0,1)$. Couples $(T_3 = \frac{-1}{2})$ $\tilde{\bar{d}}_4^{c*} \in \tilde{f}^{u\dagger}$ to $(T_3 = \frac{1}{2})$ $\tilde{\bar{d}}_4^c \in \tilde{f}^d$.

3. Higgs sector

$$y^{u\bar{u}} = \begin{pmatrix} y_{33} & y_{34} & 0\\ y_{43} & y_{44} & 0\\ 0 & 0 & 0 \end{pmatrix} \quad \text{and} \quad y^{d\bar{d}} = \begin{pmatrix} y_{\mathrm{bot}} & 0\\ 0 & 0 \end{pmatrix}.$$

APPENDIX D: BETA FUNCTIONS

1. Gauge Couplings

The beta function for the gauge couplings are

$$16\pi^2 \frac{dg_i}{dt} = -b_i g_i^3.$$

Here, $t = \ln Q$ where Q is the renormalization scale. The beta function coefficients for an arbitrary number of SU(5) multiplets n_5 and n_{10} are given by

$$b1 = \frac{3}{5}(11) + n_{10}b_{10} + n_5 b_5$$
$$b2 = 1 + n_{10}b_{10} + n_5 b_5$$
$$b3 = -3 + n_{10}b_{10} + n_5 b_5$$

with $b_{10} = 3$, $b_5 = 1$ denoting group theoretic coefficients.

2. Top Yukawa coupling

Using the general results in [53], we obtain the following top Yukawa two-loop beta function:

$$\beta_{Y_u}(t) = \frac{1}{16\pi^2}\left((3\mathrm{Tr}[Y_u(t).Y_u^\dagger(t)]Y_u(t) + 3Y_u(t)Y_u^\dagger(t)Y_u(t) + Y_u(t)Y_d^\dagger(t)Y_d(t)) - \left(\frac{16}{3}g_3(t)^2 + 3g_2(t)^2 + \frac{13}{15}g_1(t)^2\right)Y_u(t)\right).$$

Here, Y_u is the up-type Yukawa coupling matrix containing y_{33}, y_{34}, y_{43} and y_{44}.

APPENDIX E: CALCULATION OF OBLIQUE PARAMETERS

1. Fermion contribution

In [54], the authors derived a general formula for computing the values of S and T for any model with vectorlike quarks, where the number of up and down quarks are arbitrary and not necessarily equal. Adapting these general results to our model, we get

$$\begin{aligned}
T_f = \frac{3}{16\pi\sin^2\theta_W\cos^2\theta_W}\Bigg(&\sum_{\alpha=1}^{3}\sum_{i=2}^{2}([(K_L^{ud})_{\alpha i}^2 + (K_R^{\bar{u}\bar{d}})_{\alpha i}^2]\theta_+(y_\alpha, y_i) + 2[(K_L^{ud})_{\alpha i}(K_R^{\bar{u}\bar{d}})_{\alpha i}]\theta_-(y_\alpha, y_i)) \\
&- \sum_{\beta<\alpha}([(K_L^{uu})_{\alpha\beta}^2 + (K_R^{\bar{u}\bar{u}})_{\alpha\beta}^2]\theta_+(y_\alpha, y_\beta) + 2[(K_L^{uu})_{\alpha\beta}(K_R^{\bar{u}\bar{u}})_{\alpha\beta}]\theta_-(y_\alpha, y_\beta)) \\
&- \sum_{j<i}([(K_L^{dd})_{ij}^2 + (K_R^{\bar{d}\bar{d}})_{ij}^2]\theta_+(y_i, y_j) + 2[(K_L^{dd})_{ij}(K_R^{\bar{d}\bar{d}})_{ij}]\theta_-(y_i, y_j))\Bigg), \\
S_f = \frac{3}{2\pi}\Bigg(&\sum_{\alpha=1}^{3}\sum_{i=2}^{2}([(K_L^{ud})_{\alpha i}^2 + (K_R^{\bar{u}\bar{d}})_{\alpha i}^2]\psi_+(y_\alpha, y_i) + 2[(K_L^{ud})_{\alpha i}(K_R^{\bar{u}\bar{d}})_{\alpha i}]\psi_-(y_\alpha, y_i)) \\
&- \sum_{\beta<\alpha}([(K_L^{uu})_{\alpha\beta}^2 + (K_R^{\bar{u}\bar{u}})_{\alpha\beta}^2]\chi_+(y_\alpha, y_\beta) + 2[(K_L^{uu})_{\alpha\beta}(K_R^{\bar{u}\bar{u}})_{\alpha\beta}]\chi_-(y_\alpha, y_\beta)) \\
&- \sum_{j<i}([(K_L^{dd})_{ij}^2 + (K_R^{\bar{d}\bar{d}})_{ij}^2]\chi_+(y_i, y_j) + 2[(K_L^{dd})_{ij}(K_R^{\bar{d}\bar{d}})_{ij}]\chi_-(y_i, y_j))\Bigg)
\end{aligned}$$

where the K's are the generalized CKM matrices for fermions, derived in Appendix B. The greek indices sum over the up-type quark generations (i.e. from 1 to 3) and the latin indices sum over the number of down-type quark generations (i.e. from 1 to 2). The functions $\theta_\pm(y_1, y_2)$, $\psi_\pm(y_1, y_2)$ and $\chi_\pm(y_1, y_2)$ are defined in Appendix F, and $y_i \equiv m_i^2/m_Z^2$.

2. Scalar contribution

The scalar partners also contribute to the oblique corrections. For this calculation, we use the notation and conventions of [55], where the oblique parameters S and T are defined as

$$\begin{aligned}
S_s &= \frac{4\sin^2\theta_W\cos^2\theta_W}{\alpha m_Z^2}\left(\Pi_{ZZ}(m_Z^2) - \Pi_{ZZ}(0) - \frac{\cos^2\theta_W}{\cos\theta_W\sin\theta_W}\Pi_{Z\gamma}(m_Z^2) - \Pi_{\gamma\gamma}(m_Z^2)\right) \\
T_s &= \frac{1}{\alpha}\left(\frac{\Pi_{WW}(0)}{m_W^2} - \frac{\Pi_{ZZ}(0)}{m_Z^2}\right)
\end{aligned}$$

where the Π's are the electroweak vector boson self-energies. The contributions to the self-energies of the vector bosons from the additional scalars $\tilde{t}'_{1,2,3,4}$ and $\tilde{b}'_{1,2}$ are [56]

$$\Delta\Pi_{\gamma\gamma} = \frac{3}{16\pi^2} g^2 \sin^2\theta_W \left(\left(\frac{2}{3}\right)^2 \sum_{i=3}^{6} F(\tilde{t}'_i, \tilde{t}'_i) + \left(\frac{1}{3}\right)^2 \sum_{i=3}^{4} F(\tilde{b}'_i, \tilde{b}'_i) \right)$$

$$\Delta\Pi_{Z\gamma} = \frac{3}{16\pi^2} g \sin\theta_W \left(\frac{2}{3} \sum_{i=3}^{6} (\tilde{G}^Z_u)_{ii} F(\tilde{t}'_i, \tilde{t}'_i) + \frac{1}{3} \sum_{i=3}^{4} (\tilde{G}^Z_d)_{ii} F(\tilde{b}'_i, \tilde{b}'_i) \right)$$

$$\Delta\Pi_{ZZ} = \frac{3}{16\pi^2} \left(\sum_{i,j=3}^{6} |(\tilde{G}^Z_u)_{ij}|^2 F(\tilde{t}'_i, \tilde{t}'_j) + \sum_{i,j=3}^{4} |(\tilde{G}^Z_d)_{ij}|^2 F(\tilde{b}'_i, \tilde{b}'_j) \right)$$

$$\Delta\Pi_{WW} = \frac{3}{16\pi^2} \sum_{i=3}^{6} \sum_{j=3}^{4} |(\tilde{G}^W_{ud})_{ij}|^2 F(\tilde{b}'_i, \tilde{t}'_j)$$

where the $\tilde{G}$'s are the coupling matrices for scalars derived in Appendix B and the function $F(x, y)$ is given in Appendix F.

APPENDIX F: USEFUL FUNCTIONS

The expressions for $\theta_\pm(y_i, y_j)$, $\psi_\pm(y_i, y_j)$ and $\chi_\pm(y_i, y_j)$, used in Appendix E, are [57]

$$\theta_+(y_i, y_j) = y_i + y_j - \frac{2y_i y_j}{y_i - y_j} \ln\frac{y_i}{y_j}$$

$$\theta_-(y_i, y_j) = 2\sqrt{y_i y_j} \left(\frac{y_i + y_j}{y_i - y_j} \ln\frac{y_i}{y_j} - 2 \right)$$

$$\psi_+(y_i, y_j) = \frac{1}{3} - \frac{1}{9} \ln\frac{y_i}{y_j}$$

$$\psi_-(y_i, y_j) = -\frac{y_i + y_j}{6\sqrt{y_i y_j}}$$

$$\chi_+(y_i, y_j) = \frac{5(y_i^2 + y_j^2) - 22 y_i y_j}{9(y_i + y_j)^2} + \frac{3y_1 y_2 (y_i + y_j) - y_i^3 - y_j^3}{3(y_i - y_j)^3} \ln\frac{y_i}{y_j}$$

$$\chi_-(y_i, y_j) = -\sqrt{y_i y_j} \left(\frac{y_i + y_j}{6 y_i y_j} - \frac{y_i + y_j}{(y_i - y_j)^2} + \frac{2 y_i y_j}{(y_i + y_j)^3} \ln\frac{y_i}{y_j} \right).$$

Here, $y_i = m_i^2/m_Z^2$, $y_i = m_i^2/m_Z^2$ and the limit $\epsilon \to 0$ of dimensional regularization is assumed. The expression for $F(x, y)$ in the self-energy functions in Appendix E is [56]

$$F(x, y) = H(x, y) + (x + y - p^2) B(x, y)$$

$$H(x, y) = (2p^2 - x - y - (x - y)^2/p^2) B(x, y)/3 + (x \overline{\ln} x + m_y^2 \overline{\ln} y - p^2/3 + (x \overline{\ln} x - x - y \overline{\ln} y + y)(y - x)/(2p^2))2/3$$

$$B(x, y) = -\int_0^1 dt \overline{\ln}(tx + (1 - t)y - t(1 - t)p^2 - i\epsilon),$$

where now $x = m_x^2$, $y = m_y^2$ and $\overline{\ln} X = \ln(X/m_Z^2)$.

[1] ATLAS Collaboration, Report No. ATLAS-CONF-2012-093, 2012, http://cdsweb.cern.ch/record/1460439.

[2] CMS Collaboration, Report No. CMS-PAS-HIG-12-020, 2012, http://cdsweb.cern.ch/record/1460438.

[3] R. Barbieri and A. Strumia, arXiv:hep-ph/0007265.

[4] G. F. Giudice and R. Rattazzi, Nucl. Phys. **B757**, 19 (2006).

[5] M. A. Luty, arXiv:hep-th/0509029.

[6] L. M. Carpenter, D. E. Kaplan, and E.-J. Rhee, Phys. Rev. Lett. **99**, 211801 (2007).

[7] L. M. Carpenter, D. E. Kaplan, and E. J. Rhee, arXiv:0804.1581.

[8] P. W. Graham, D. E. Kaplan, S. Rajendran, and P. Saraswat, J. High Energy Phys. 07 (2012) 149.

[9] J. Fan, M. Reece, and J. T. Ruderman, J. High Energy Phys. 11 (2011) 012.
[10] G. D. Kribs and A. Martin, Phys. Rev. D **85**, 115014 (2012).
[11] M. Baryakhtar, N. Craig, and K. Van Tilburg, J. High Energy Phys. 07 (2012) 164.
[12] R. Dermisek, Mod. Phys. Lett. A **24**, 1631 (2009).
[13] K. Choi, K. S. Jeong, T. Kobayashi, and K. i. Okumura, Phys. Lett. B **633**, 355 (2006).
[14] R. Kitano and Y. Nomura, Phys. Lett. B **631**, 58 (2005).
[15] Z. Chacko, Y. Nomura, and D. Tucker-Smith, Nucl. Phys. **B725**, 207 (2005).
[16] J. R. Ellis, J. F. Gunion, H. E. Haber, L. Roszkowski, and F. Zwirner, Phys. Rev. D **39**, 844 (1989).
[17] J. R. Espinosa and M. Quiros, Phys. Rev. Lett. **81**, 516 (1998).
[18] P. Batra, A. Delgado, D. E. Kaplan, and T. M. P. Tait, J. High Energy Phys. 02 (2004) 043.
[19] A. Maloney, A. Pierce, and J. G. Wacker, J. High Energy Phys. 06 (2006) 034.
[20] J. A. Casas, J. R. Espinosa, and I. Hidalgo, J. High Energy Phys. 01 (2004) 008.
[21] A. Brignole, J. A. Casas, J. R. Espinosa, and I. Navarro, Nucl. Phys. **B666**, 105 (2003).
[22] R. Harnik, G. D. Kribs, D. T. Larson, and H. Murayama, Phys. Rev. D **70**, 015002 (2004).
[23] S. Chang, C. Kilic, and R. Mahbubani, Phys. Rev. D **71**, 015003 (2005).
[24] A. Delgado and T. M. P. Tait, J. High Energy Phys. 07 (2005) 023.
[25] A. Birkedal, Z. Chacko, and Y. Nomura, Phys. Rev. D **71**, 015006 (2005).
[26] K. S. Babu, I. Gogoladze, and C. Kolda, arXiv:hep-ph/0410085.
[27] K. Choi, K. S. Jeong, T. Kobayashi, and K. i. Okumura, Phys. Rev. D **75**, 095012 (2007).
[28] R. Dermisek and H. D. Kim, Phys. Rev. Lett. **96**, 211803 (2006).
[29] H. Abe, T. Kobayashi, and Y. Omura, Phys. Rev. D **76**, 015002 (2007).
[30] M. Dine, N. Seiberg, and S. Thomas, Phys. Rev. D **76**, 095004 (2007).
[31] H. Abe, Y. G. Kim, T. Kobayashi, and Y. Shimizu, J. High Energy Phys. 09 (2007) 107.
[32] B. Dutta, Y. Mimura, and D. V. Nanopoulos, Phys. Lett. B **656**, 199 (2007).
[33] T. Kikuchi, arXiv:0812.2569.
[34] S. G. Kim, N. Maekawa, A. Matsuzaki, K. Sakurai, A. I. Sanda, and T. Yoshikawa, Phys. Rev. D **74**, 115016 (2006).
[35] B. Dutta and Y. Mimura, Phys. Lett. B **648**, 357 (2007).
[36] B. Bellazzini, C. Csaki, A. Delgado, and A. Weiler, Phys. Rev. D **79**, 095003 (2009).
[37] I. Gogoladze, M. U. Rehman, and Q. Shafi, Phys. Rev. D **80**, 105002 (2009).
[38] P. W. Graham, A. Ismail, S. Rajendran, and P. Saraswat, Phys. Rev. D **81**, 055016 (2010).
[39] S. P. Martin, Phys. Rev. D **81**, 035004 (2010).
[40] G. Burdman, Z. Chacko, H. S. Goh, and R. Harnik, J. High Energy Phys. 02 (2007) 009.
[41] Z. Chacko, H. S. Goh, and R. Harnik, Phys. Rev. Lett. **96**, 231802 (2006).
[42] S. Chang, L. J. Hall, and N. Weiner, Phys. Rev. D **75**, 035009 (2007).
[43] A. Falkowski, S. Pokorski, and M. Schmaltz, Phys. Rev. D **74**, 035003 (2006).
[44] N. Arkani-Hamed, A. G. Cohen, E. Katz, and A. E. Nelson, J. High Energy Phys. 07 (2002) 034.
[45] N. Arkani-Hamed, A. G. Cohen, and H. Georgi, Phys. Lett. B **513**, 232 (2001).
[46] S. P. Martin and J. D. Wells, Phys. Rev. D **86**, 035017 (2012).
[47] J. A. Aguilar-Saavedra, R. Benbrik, S. Heinemeyer, and M. Perez-Victoria, Phys. Rev. D **88**, 094010 (2013).
[48] CMS Collaboration, Phys. Lett. B **729**, 149 (2014).
[49] M. E. Peskin and T. Takeuchi, Phys. Rev. Lett. **65**, 964 (1990).
[50] A. Ceccucci, Z. Ligeti, and Y. Sakai (Particle Data Group), CKM quark-mixing matrix, 2012.
[51] ATLAS Collaboration, Report No. ATLAS-CONF-2013-051.
[52] J. Beringer *et al.* (Particle Data Group), Phys. Rev. D **86**, 010001 (2012).
[53] S. P. Martin and M. T. Vaughn, Phys. Rev. D **50**, 2282 (1994); **78**, 039903(E) (2008).
[54] L. Lavoura and J. P. Silva, Phys. Rev. D **47**, 2046 (1993).
[55] S. Eidelman *et al.* (Particle Data Group Collaboration), Phys. Lett. B **592**, 1 (2004).
[56] S. P. Martin, K. Tobe, and J. D. Wells, Phys. Rev. D **71**, 073014 (2005).
[57] L. Lavoura and J. P. Silva, Phys. Rev. D **47**, 1117(1993).